1

Study of disintegrability in compost and enzymatic degradation of PLA and PLA

nanocomposites reinforced with cellulose nanocrystals extracted from *Posidonia Oceanica*

3

4 F. Luzi, E. Fortunati[*], D. Puglia, R. Petrucci, J.M. Kenny, L. Torre

5

6 University of Perugia, Civil and Environmental Engineering Department, UdR INSTM, Strada di

7 Pentima 4, 05100 Terni (Italy)

8

9 [*]**Corresponding author**: Tel.: +39-0744492921; fax: +39-0744492950; E-mail address:

10 elena.fortunati@unipg.it (E. Fortunati)

11

12 **Abstract**

13 Nanocomposite films based on poly(lactic acid) (PLA) reinforced with cellulose nanocrystals

14 extracted from *Posidonia Oceanica* plant were prepared by solvent casting method containing 1 or

15 3 %wt of cellulose nonocrystals unmodified (CNC) and modified using a commercial surfactant (s-

16 CNC). The modification improves the dispertion of CNC into the matrix. Enzymatic degradation

17 using efficient enzyme proteinase K and disintegrability in composting conditions were considered

18 to gain insights into the post-use degradation processes of the produced formulations. Results of

19 visual, morphological and thermal analysis of enzymatic degradation studies confirmed that the

20 selected enzyme preferentially degraded amorphous regions with respect of crystalline ones, while

21 the crystallinity degree of the nanocomposite films increased during enzymatic degradation, as a

22 consequence of enzyme action. The disintegration in compositing conditions of different

23 formulations was also investigated by means of visual and morphological analysis. The

24 disintegrability in compost conditions showed that the formulations disintegrated in less than 14

25 days, in addition it has been proved that CNC modified with surfactant were able to promote the

26 disintegration behaviour. The production of PLA based nanocomposites incorporating cellulose

extract from marine wastes suggested the potential application of the proposed material for short-term food packaging with low enviromental impact.

1. Introduction

In the last years, biodegradable polymers, that can be decomposed by fungal or microoorganisms, have been considered as promising alternative to petrochemical-based polymers for specific applications [1].

Every year, 140 million tons of petroleum based polymers are produced and introduced in the ecosystem as industrial waste products [2]. Biodegradable polymers are based on renewable materials, such as starch, lignin, cellulose etc., or synthesized from renewable resources. The green materials have a lower negative environmental impact than the petroleum based materials. Poly (lactic acid) (PLA) is one of the most attractive green plastic useful for the production of ecofriendly food packaging [3], it can be degraded into CO_2 and H_2O [4]. It is a linear aliphatic thermoplastic polyester derived from renewable resources such as fermentation of starch and other polysaccharides [5] like corn, rice and sugar beets [6]. PLA is a biocompatible, biodegradable and crystalline polymer, the products manufactured usising this matix completely disintegrated in less than one month in ideal conditions or in specific medium or environments [7]. Moreover, PLA can be processed by injection molding, film extrusion, blow molding, thermoforming, fiber spinning, and film forming and has better thermal processability in comparison with other biopolymers, such as poly (ε-caprolactone)(PCL), poly(hydroxyl alkanoates) (PHAs), etc. [8, 9].

The properties of PLA are dependent on the ratio of D and L enantiomers [10]. It exhibits interesting physical [1] and functional properties as good transparency, good mechanical properties and low cost.

PLA is approved by the Food and Drug Administration (FDA) and can be used in biomedical application, in direct contact with biological fluids and for implantation in the human body and does not produce toxic components [11] or carcinogenic effects in local tissues [8] during the degradation into the body [12]. However, PLA matrix exhibits some limitations when it is used in food applications compared to equivalent traditional polymers, as lower barrier properties

3

(important properties for food packaging), high brittleness, slow crystallization rate and relatively low thermal and mechanical properties [13]. In order to overcome these limitations, several strategies can be adopted to decrease and modulate these properties. The development of nanocomposites or blends represents a valid solution to modify the initial characteristics. The production of nanocomposites reinforced with nanofiller extracted from natural resources is a valid strategy used to increase the physical properties of renewable and biodegradable polymers, without affecting their transparency properties.

Cellulose nanocrystals have received, in the last period, a big interest as natural reinforcement able to increase the properties of a biomaterial suitable for food packaging applications [14]. Moreover, CNC present excellent biocompatibility [15], high stiffness and low density [16]. CNC can be extracted from different natural resources as *Cynara Cardunculus* [17], bamboo [18], phormium, flax [19] and other natural sources and waste [20, 21]. The obtained nanostructures are usually characterized by rigid rod monocrystalline domains with diameters ranging from 1-100 nm and from ten to hundreds of nm in length [22]. In general, the nanocrystals aspect ratio (diameter/length) can vary from 1:1 to 1:100 and the dimensions of the CNC depend on the raw material utilized for their extraction [23] and the intensity of the chemical process for their production [24]. CNC have a crystalline structure [25] and an elastic modulus around 150 GPa [26].

In this research, CNC extracted from *Posidonia Oceanica* ball wastes have been used. This aquatic plant appears on Mediterranean coastal beaches in big amounts in the form of balls as a consequence of storms that tear off leaves and stems in some cases [27], consequently, the plants have to be removed to maintain the optimum condition of the coastal for the tourists. Several academic research have focused their attention on the revalorization of ligno-cellulosic wastes of *Posidonia Oceanica* plant [28-30] as reinforcement or nanoreinforcement in different matrices for bio-based films [31, 32] or as filler for traditional polymer [27].

Recently, Fortunati et al. 2015 [32] reported the preparation of CNC extracted from *Posidonia Oceanica* balls; in the same research, they also presented the production and the characterization of

4

1 PLA based nanocomposites reinforced with cellulose nanocrystals unmodified (CNC) and modified

2 (s-CNC) with a surfactant.The use of surfactant is a valid strategy to improve the dispersion of the

3 CNC in a polymeric matrix [33]. The positive results obtained by functional, optical and migration

4 properties of PLA based films suggested the possibility of using these bio-based nanocomposites in

5 industrial application.

6 In the present work, enzymatic degradation and disintegrability in composting conditions of PLA

7 nanocomposites reinforced with both unmodified and surfactant modified cellulose nanocrystals

8 extracted from *Posidonia Oceanica* balls have been tested, in order to evaluate the post-use

9 behaviour of these potential food packaging systems. The disintegrability in compost was carried

10 out at 58 °C in aerobic condition and 50 % of humidity.

11 The enzyme selected for the enzymatic degradation test, a protease from *Tritirachium album*,

12 proteinase K, was found to be able to degrade selectively L-lactic bonds and not the D-lactic ones,

13 being poly(D- lactic) not degradable with this specific enzyme [34, 35]. The enzyme shows the

14 major effect on degradation in amorphous region respect to crystalline ones [35-37]. In fact as

15 previously reported in literature the degradation rates of PLA decreased with an increase in

16 crystallinity [38].

17 Visual observation and morphological analysis were performed at different times for each test, with

18 the aim of evaluating how the two different procedures influenced the properties of the films.

19 Moreover, thermal analysis was carried out only for film tested in enzymatic degradation

20 conditions, in order to highlight how proteinase K selectively degraded amorphous regions with

21 respect of crystalline ones.

22

23 **2.Experimental section**

24 **2.1 Materials**

25 Poly(lactic acid) (PLA) in forms of fibres (specific gravity 1.25 g cm^{-3}, 6 mm length), was supplied

26 by MiniFibers, Inc..

1 *Posidonia Oceanica* waste balls were collected from the Campello Beach in Alicante (Spain), by

2 Aitex (Alcoy, Alicante, Spain). *Posidonia Oceanica* is a Mediterranean endemic alga characterized

3 by relatively high amounts of extractives. The preparation of the cellulose nanocrystals (CNC)

4 extracted from *Posidonia Oceanica* was previously described [32]. Briefly, the extraction procedure

5 of cellulose nanocrystals was implemented in two steps (Figure 1). The first step, a chemical alkali

6 treatment, leads to the production of holocellulose by the gradual removal of lignin, while the

7 subsequent sulphuric acid hydrolysis process allows obtaining cellulose nanocrystals in an aqueous

8 suspension from *Posidonia Oceanica* wastes. The mean diameter of the unbleached fibres was

9 84 ± 26 μm, however, after bleaching pre-treatments as a consequence of elimination of lignin,the

10 fibres appeared separated and the mean diameter reduced at about 7 ± 2 μm. The CNC appear

11 individualized and with acicular rod shape, (180 ± 28) nm in length a diameter of (4.9 ± 1.3) with a

12 aspect/ratio of 36.7 [32].

13 Tris(hydroxymethyl)aminomethane/HCl,   sodium   azide,   and   proteinase   K   obtained   from

14 *Tritirachium album* (lyophilized powder, $\geq$ 30 units/mg protein) and all the chemical reagents were

15 supplied by Sigma Aldrich[®].

16

17 **2.2 PLA nanocomposite processing**

18 PLA nanocomposite films reinforced with CNC and s-CNC were prepared by solvent casting

19 method using chloroform. Firstly, PLA (0.75 g) was dissolved in 25 mL of $CHCl_3$ with stirring at

20 room temperature (RT). Then specific amount of cellulose nanocrystals (1 wt% and 3 wt% of

21 unmodified (CNC) and modified with commercial surfactant(s-CNC)), were added, and related

22 samples, designed respectively as PLA_1CNC, PLA_3CNC, PLA_1s-CNC and PLA_3s-CNC,

23 were produced. The CNC were modified with a commercial surfactant (Beycostat A B09 - CECCA

24 S.A.) [39], an acid phosphate ester of ethoxylatednonylphenol, with the aim of improving both the

25 dispersion of the nanoreinforcements into the matrix and the final properties of the nanocomposites.

26 The solution of s-CNC was prepared adding the surfactant in the proportion of 1/4 (wt/wt) directly

6

1   to the CNC aqueous solution. In order to increase the thermal stability of the produced nanocrystals,

2   the pH of CNC and s-CNC aqueous solutions was raised to approximately 9, by using a 0.25 %wt

3   NaOH solution [40].

4   The CNC in powder (unmodified and modified) was added to the $CHCl_3$, forming 1 wt%

5   suspension. The cellulose nanocrystal solution was exposed to sonication (Vibracell, 750W) for 1

6   min in an ice bath.The different solutions were cast onto a 15 cm diameter glass Petri dish and then

7   dried for 24 h at RT.

8

9   **2.3 Disintegrability in composting of PLA and PLA nanocomposites**

10   Disintegrability in composting conditions was carried out following the European standard ISO

11   20200. The test method determines, at laboratory-scale, the degree of disintegration of plastic

12   materials under simulated intensive aerobic composting condition [41]. This method studies the

13   disintegration and not the biodegradability of plastic materials. The degree of disintegration D was

14   calculated in percent by normalizing the sample weight at different days of incubation to the initial

15   weight by using Equation (1):

16   $$D = \frac{m_i - m_r}{m_i} * 100 \qquad \text{(Eq. 1)}$$

17   where:

18   m_i= is the initial dry plastic mass;

19   m_r= is the dry plastic material after the test.

20   PLA and PLA nanocomposite films of dimension 15 mm x 15 mm x 0.03 mm were weighed and

21   buried into the organic substrate at 4-6 cm depth in the perforated boxes guarantying the aerobic

22   conditions and incubated at 58 ºC at 50 % of humidity. The aerobic conditions were guaranteed by

23   mixing periodically the solid soil. The materials tested can be considered disintegrable according to

24   the European standard when 90% of the plastic sample weight shall be lost within 90 days of

25   analysis. In order to simulate the disintegrability in compost, a solid synthetic waste was prepared,

mixing sawdust, rabbit food, compost inoculum supplied by Genesu S.p.a., starch, sugar, oil and urea. The water content of the substrate was around 50 % and the aerobic condition was guaranteed into the boxes by hand mixing the materials every day. The different formulations were tested for maximum 14 days. The samples tested were taken out at different times (1, 3, 7, 10 and 14 days), washed with distilled water and dried in a oven at 37 °C for 24 h.

The photographs on the samples were taken for visual comparison,while the surface microstructure of the PLA and PLA nanocomposites was investigated, before and after 3 days of incubation, by means of a field emission scanning electron microscope (FESEMSupra 25-Zeiss), after gold sputtering of the samples.

2.4 Enzymatic degradation of PLA and PLA nanocomposites

For enzymatic degradation analysis, each sample was cut with dimensions of 15 x 15 x 0.03 mm, and weighed before its immersion in the degradation medium. After that, the samples were placed in vials filled with degradation medium formed by the enzyme (0.5 mg) and 5 mL of tris(hydroxymethyl)aminomethane/HCl buffer (0.05 M, pH 8.6), to optimize the enzyme activity. Sodium azide (0.02 wt %) was added to each buffer solution to inhibit the growth of microorganisms. Enzymatic degradation was performed in an incubator at 37 ºC and the buffer-enzyme system was renewed every 24 hours for 21 days to maintain the enzymatic activity. Specimens (in triplicate) of each formulation were removed for the different time selected for this study. The samples tested were taken out at 2, 6, 18 and 24 hours and at 1, 2, 3, 5, 7, 8, 9, 16 and 21 days, washed with distilled water and dried at room temperature up to constant weight.

Weight measurements, determined using an analytical balance (± 0.00001 g), and visual observations, were performed for each specimen. The weight loss (WL) of the samples was evaluated by using by using Equation (2):

$$WL(\%) = \frac{(W_0 - W_t)}{W_0} * 100 \qquad \text{(Eq. 2)}$$

where:

W_0= is the initial dry plastic mass;

W_t= is the dry weight of a material after enzymatic degradation.

Another important parameter to be considered is the water absorption (WA) during the degradation process, the hydrophilic polymers take up water and the degradation rate increase [42]. It was calculated by using Equation (3):

$$WA(\%) = \frac{(W_w - W_t)}{W_t} * 100 \qquad \text{(Eq. 3)}$$

where:

W_w= is the weight of plastic material after enzymatic degradation;

W_t= is the dry weight of a material after enzymatic degradation.

Thermal characterization after enzymatic degradation was performed using differential scanning calorimetry (DSC) and thermogravimetric analysis (TGA) at different incubation times.Differential scanning calorimeter (DSC, Mettler Toledo 822/e) investigations were done from -25 to 210°C, at 10 °C min^{-1}, applying two heating and one cooling scans in nitrogen atmosphere (50mL min^{-1}). Melting and cold crystallization temperatures and enthalpies (T_m, T_{cc} and ΔH_m, ΔH_{cc}) were determined from the first and second heating scan, while crystallization phenomena were analyzed during the cooling scan. The glass transition temperature (T_g) was registered for each scan. Three samples were used to characterize each formulation.

The crystallinity degree was calculated by using Equation (4):

$$\chi = \frac{1}{(1 - m_f)} \left[\frac{(\Delta H_m - \Delta H_{cc})}{\Delta H_0} \right] * 100 \qquad \text{(Eq. 4)}$$

where ΔH_m is the melt enthalpy and ΔH_{cc} is the cold crystallization enthalpy, ΔH_0 is enthalpy of melting for a 100% crystalline PLA sample, taken as 93 J g^{-1} [43], mf is the weight fraction of nanoreinforcements in the sample and (1-m_f) is the weight fraction of PLA in the sample.

1   Thermogravimetric analysis (TGA - Seiko Exstar 6300) from 30 to 600 °C at 10 °C min^{-1} under a

2   nitrogen atmosphere (250 mL min^{-1}) on 10 mg weight was performed for each sample.

3   Finally, the surface microstructure of the PLA nanocomposites before and after enzymatic

4   degradation at different incubation times was investigated by FESEM.

5

6   **2.5 Statistical analysis**

7   Statistical analysis of data was performed through analysis of variance (ANOVA) using

8   Statgraphics Plus for Windows 5.1 Program (Munugistics Corp., Rockville, MD). Fisher's least

9   significant difference (LSD) was used at the 95% confidence.

10

11   **3. Results and Discussion**

12   **3.1 Disintegrability in composting conditions of PLA and PLA nanocomposites**

13   The disintegrability in composting conditions of PLA and PLA based nanocomposites represents an

14   interesting and attractive property for packaging applications that simulate the post-use of plastics

15   [44, 45]. Composting is a natural process, in which the organic material can be decomposed by

16   microorganisms, including fungi and bacteria. PLA degradation starts with diffusion of water into

17   the materials. The hydrolysis of PLA produces a molecular weight reduction by random non-

18   enzymatic chain scissions of the ester groups, leading to the formation of oligomers and lactic acid.

19   The disintegrability in composting made by microorganisms such as fungi and bacteria starts when

20   the molecular weight of PLA reaches about 10.000-20.000 g mol^{-1}. The microorganisms metabolize

21   the macromolecules as organic matter, converting them to carbon dioxide, water and humus [44].

22   The use of nanoparticles, as nanoreinforcements, influence the biodegradation in compost of PLA

23   and the disintegrability process strongly depends on their hydrophilicity and their nature [46, 47].

24   Figure 2 shows the visual observation (Figure 2,a) and the disintegrability values (Figure 2,b) of the

25   PLA samples reinforced with both unmodified and surfactant modified CNC extracted from

26   *Posidonia Oceanica* taken out at different times of composting. The disintegrability value was

evaluated in terms of weight loss as a function of testing time, in which the line at 90 % of disintegration represents the limit point of disintegrability imposed by the ISO 20200; Figure 2,b shows that all the materials reach a degree of disintegration exceeding 90% after 14 days of composting, showing an evident visual fragmentation. After only one day of incubation, the samples start to change their appearance, as it is possible to see in Figure 2,a: the formulations appear white and deformed and this effect is more evident after 3 days in composting conditions. The whitening process and the formulation opacity are attributed to change in the refractive index due to water absorption, with the formation of low molecular weight compounds [47], the creation of some holes on the materials and an induced increase of the crystallinity during degradation [48]. Moreover, after 3 days of incubation, PLA_3s-CNC film became breakable respect to the other samples, due to the different morphology of the cross section that characterized this sample, as reported by Fortunati et al 2015 [32]. The cross section of PLA_3s-CNC system, in fact, appears characterized by a porous structure induced by the presence of the surfactant. The presence of the pores favors the process of disintegrability in composting since the internal structure is easily accessible by water and microorganisms. After 7 days of incubation, the films became breakable and the weight loss considerably increases; the PLA_CNC formulations show a reduction in weight of 30-40%, while the PLA_s-CNC based systems show a higher reduction, reaching a 70% of disintegrability for the film reinforced with 3 %wt of cellulose nanocrystals. This different behaviour is correlated to the different morphology of cross sections and to the presence of hydrophilic surfactant in PLA_s-CNC based nanocomposites. The lower disintegration rate obtained for PLA_CNC was attributed to the cellulose nanocrystal introduction that, increasing the crystallinity of the systems, affects the water diffusion through the PLA matrix and, consequently, the disintegration kinetics [45]. The addition of hydrophilic cellulose is expected to accelerate the degradation rate in PLA nanocomposites, but at the same time CNC could also inhibit water diffusion, thus explaining the obtained results [49].

1   Figure 3 shows the FESEM images of the neat PLA and PLA nanocomposites surfaces before and

2   after 3 days in composting conditions. After 3 days at 58 °C, a clear surface erosion with the

3   appearance of holes and porous structures on PLA and all PLA nanocomposites was observed,

4   particularly visible in the PLA_3s-CNC samples [50, 51]. Moreover, the disintegrability experiment

5   took place at 58 °C, temperature higher of the nanocomposite glass transition temperature (T_g)

6   (Table 1 time 0). The higher temperature and the surfactant presence are able to increase the chain

7   mobility [45] facilitating the formation of pores structures on the sample surfaces. The breakable

8   structure facilitates the polymer erosion by microorganisms attack. The erosion surface after 3 days

9   was no so evident for the CNC based systems, confirming the potentiality of the cellulose crystals

10   to induce the crystallization of PLA polymer and to inhibit the diffusion process acting by barrier

11   agents [52, 53].

12

13   **3.2 Enzymatic degradation of PLA and PLA nanocomposites**

14   Figure 4 shows the images of different films (Figure 4,a,b- Panel A) and weigh loss curves (Figure

15   4,a-b - Panel B) of the studied samples as a function of different degradation times. After 6 hours of

16   incubation, the samples start to change, as it is possible to see by visual observation (Figure 4,a); the

17   transparency clearly decreases and all the formulations appear opaque, white and deformed. After

18   24 hours in the medium, PLA and PLA nanocomposites show a linear increase of the weight loss. It

19   was observed a higher degradation for PLA neat films with respect to PLA nanocomposites. After

20   only 24 hours of incubation, the PLA showed up to (88.3±1.4) % of weight loss. These results

21   confirm that PLA degradation is catalysed by proteinase K [35, 54]. On the other hand, PLA and

22   PLA reinforced with CNC appeared degraded after 6 hours of test reaching 40-60 % of degradation

23   while PLA reinforced with s-CNC maintained the weight loss lower to 10 % (Figure 4 a, Panel B).

24   Specifically, the weight loss of neat PLA is (88.3±1.4)% after 24 h, followed by PLA_1CNC

25   (69.0±0.9) %, PLA_3CNC (63.2±3.7) %, while the weight loss is (16.6±1.3) % and (23.1±2.3) %,

26   for PLA_1-s-CNC and PLA_3-s-CNC, respectively.

The different behaviour that characterizes the CNC and s-CNC based formulations can be attributed to the presence of surfactant. In detail, we notice that the surfactant, an acid phosphate ester of ethoxylatednonyl phenol, is able to decrease the pH level of the aqueous solution (pH = 4-5) inhibiting the action of the enzyme that needs a pH ranged from 7.5 to 12 to explain its action [35, 41, 55].

Figure 5 shows the water absorption during the first 24 hours (Figure 5, a) till to 21 days (Figure 5, b). All the formulations reach the saturation limit of water absorption after 18 hours in contact with the enzyme containing solution. The formulations reinforced with s-CNC show higher water absorption values; this behaviour can be related to the presence of micro-holes, basically due to the presence of the hydrophilic surfactant used to improve the dispersion of CNC into the matrix, as previously reported [32].

FESEM images of the samples, at different incubation times during enzymatic degradation, are reported in Figure 6. After 2 hours, a change in the system morphologies was observed. A clear surface erosion with several and tiny holes and channels on PLA and PLA_CNC surfaces are observed. A similar result about morphological investigation was previously obtained by Malwela et Ray (2015) in the enzymatic degradation study of PLA/PBSA blend composites [55]. The surface modification and the presence of holes and the porous structures can be due to the degradation of the amorphous region eroded preferentially by proteinase K [35, 56]. This effect is not so evident in the case of PLA_s-CNC based formulations, that maintain their original topography till 24 h of incubation with the enzyme. A more evident surface erosion for PLA_s-CNC based formulations is visible after 3 and 7 days in contact with the enzyme containing solution in accord with the slower degradation kinetic detected by the weight loss measurements previously discuss.

3.2.1 Thermal properties of PLA nanocomposites after enzymatic degradation

The thermal properties of PLA and PLA nanocomposites at different incubation times are investigated by TGA and DSC. The derivative curves of the mass loss (DTG) for the different

studied formulations are reported in Figure 7, while the DSC thermal properties are summarized in Table 1 and Figure 8 (first heating scans for all the materials).

Thermogravimetric analysis (Figure 7) of PLA revealed a reduction of the main peak temperature (temperature of maximum degradation rate) that shifts of about 20 °C to lower temperature, after only 2 hours in contact with the enzyme (Figure 7, a). Moreover, the PLA maximum degradation temperature shifts from 332 °C to 278 °C after 2 days of incubation (2 days represent the last time for PLA enzymatic degradation). A different behaviour is detected for PLA reinforced with unmodified and modified cellulose nanocrystals. The main degradation temperature of PLA_1CNC and PLA_3CNC during the enzymatic degradation remains unmodified as previously observed in literature proving that CNC are able to improve the thermal stability of the PLA matrix (Figure 7, b,c) [44, 54]. PLA_1s-CNC and PLA_3s-CNC curves (Figure 7, d,e) show two main peaks of degradation: the first one is associated to the PLA degradation around 330 °C while the second one, at around 500 °C, is related to the surfactant degradation [40]. The variation of the main degradation peaks becomes relevant when the surfactant starts to be released from the formulations and the evidence of the surfactant release from the s-CNC based films is clearly detected in the insert of Figure 7, e. When the surfactant weight starts to decrease (reduction in the intensity of the peak at around 500 °C), also the maximum degradation peak starts to shift to lower temperature as evidence of the occurring degradation mechanism. In particular, the weight loss of PLA_1s-CNC formulation increases after 8 days in enzymatic medium and the same phenomenon is detected for PLA_3s-CNC after 2 days of incubation. As just discussed above, the presence of surfactant in the PLA nanocomposites improves the dispersion of CNC but at same time obstacles the enzyme activity modifying the pH of the medium [42]. Moreover, a higher degradation kinetics of PLA_3s-CNC with respect to the PLA_1s-CNC is observed. The degradation of PLA_3s-CNC is accelerated by the presence of several holes on the fractured surface [32] that facilitated the hydrolytic degradation of the PLA. In particular, the main peak for PLA_1-s-CNC, shifts from 330 °C to 302 °C after 21 days while PLA_3-s-CNC reaches 304 °C after only 5 days.

Figure 8 shows the DSC thermograms related to the first heating scan, underlining the variation of crystallization and melting properties at the beginning and at the end of the enzymatic degradation test. The DSC experiments are performed with the aim of investigating the thermal behaviour of PLA nanocomposites during the enzymatic degradation. As it is possible to observe, for PLA and PLA_CNC systems the peak of the cold crystallization disappears completely at the end of test, while for PLA_s-CNC based nanocomposites the peak decreases in its intensity. The melting peak of nanocomposites at initial time is characterized by the presence of two melting peaks. The first peak disappears during the degradation test as observed by thermograms and as reported in Table 1. During the first heating scan (Table 1) some changes are observed in glass transition temperature, cold crystallization temperature, melting enthalpy and cold crystallization enthalpy while for the second value of melting temperature not significant changes are detected. The cold crystallization enthalpy decreases, while the melting enthalpy increases with the time encouraging the crystallization according with literature [42]. The crystallinity degree values, calculated at time zero, are (8.9±3.4), (8.6±3.0), (7.5±1.7), (9.5±0.2) and (11.4±2.0) respectively for PLA, PLA_1CNC, PLA_3CNC, PLA_1s-CNC and PLA_3s-CNC. The same values, calculated at the final stage of the enzymatic degradation for each formulations, increased up to (35.4±0.8), (31.9±0.9), (24.5±0.7), (35.1±3.7) and (31.1±0.5) respectively for PLA, PLA_1CNC, PLA_3CNC, PLA_1s-CNC and PLA_3s-CNC. The increase in crystallinity degree highlights the action of specific enzyme able to degrade amorphous regions [35]. The increase in crystallinity degree can be correlated to the visual appearance of the sample surfaces of PLA and PLA nanocomposites: the films change the colour becoming white, opaque and deformed. Moreover, the two melting peaks of neat PLA, PLA_1CNC PLA_3CNC are associated to the coexistence of two kinds of crystalline structure of PLA [57], while this effect is not evident in the case of PLA reinforced with s-CNC.

4. Conclusions

This research involved two different studies for simulation, at laboratory scale, of the post use of nanocomposite films based on poly(lactic acid) (PLA) and cellulose nanocrystals (CNC) extracted from *Posidonia Oceanica* plant prepared by solvent casting method. The films disintegrated completely during 14 days of the test. The disintegration rate in composting condition was increased by the presence of s-CNC, due to the hydrophilicity of the surfactant. In particular, the disintegrability of PLA_3s-CNC is accelerated by the presence of holes detected by morphology study on cross section surfaces.

Proteinase K strongly catalysed the degradation of PLA and PLA nanocomposites, this effect was delayed in PLA_s-CNC based nanocomposites. This behaviour can be related to the presence of surfactant that, in enzymatic buffer, can be released changing the optimum conditions for the enzyme activity. In fact, it was observed that the degradation values in enzyme buffer for PLA_s-CNC increased with decreased presence of surfactant, as detected by thermogravimetric analysis. PLA and PLA_CNC films degraded completely in two days in enzymatic medium. Moreover, proteinase K degraded preferentially the amorphous region with respect of crystalline one. The DSC analysis confirmed the higher value of crystallinity degrees obtained during the different degradation times.

References

1. Stloukal P, Kalendová A, Mattausch H, Laske S, Holzer C, Koutny M. The influence of a hydrolysis-inhibiting additive on the degradation and biodegradation of PLA and its nanocomposites. Polym Test 2015;41:124-132.

2. Madhavan Nampoothiri K, Nair NR, John RP. An overview of the recent developments in polylactide (PLA) research. Bioresource Technol 2010;101(22):8493-8501.

3. Averous L. Biodegradable multiphase systems based on plasticized starch: A review. J Macromol Sci Polym R 2004;C44(3):231-274.

4. Arjmandi R, Hassan A, Eichhorn SJ, Haafiz MKM, Zakaria Z, Tanjung FA. Enhanced ductility and tensile properties of hybrid montmorillonite/cellulose nanowhiskers reinforced polylactic acid nanocomposites. J Mater Sci 2015;50(8):3118-3130.

5. Arrieta MP, Samper MD, López J, Jiménez A. Combined Effect of Poly (hydroxybutyrate) and Plasticizers on Polylactic acid Properties for Film Intended for Food Packaging. J Polym Environment 2014;22(2):460-470.

6. Dong Y, Ghataura A, Takagi H, Haroosh HJ, Nakagaito AN, Lau K-T. Polylactic acid (PLA) biocomposites reinforced with coir fibres: Evaluation of mechanical performance and multifunctional properties. Compos Part A-Appl S 2014;63:76-84.

7. Jonoobi M, Harun J, Mathew AP, Oksman K. Mechanical properties of cellulose nanofiber (CNF) reinforced polylactic acid (PLA) prepared by twin screw extrusion. Compos Sci Technol 2010;70(12):1742-1747.

8. Rasal RM, Janorkar AV, Hirt DE. Poly (lactic acid) modifications. Prog Polym Sci 2010;35(3):338-356.

9. Arrieta MP, López J, Hernández A, Rayón E. Ternary PLA–PHB–Limonene blends intended for biodegradable food packaging applications. Eur Polym J 2014;50(0):255-270.

10. Abdelwahab MA, Flynn A, Chiou B-S, Imam S, Orts W, Chiellini E. Thermal, mechanical and morphological characterization of plasticized PLA–PHB blends. Polym Degrad Stabil 2012;97(9):1822-1828.

11. Armentano I, Bitinis N, Fortunati E, Mattioli S, Rescignano N, Verdejo R, Lopez-Manchado MA, Kenny JM. Multifunctional nanostructured PLA materials for packaging and tissue engineering. Progr Polym Sci 2013;38(10):1720-1747.

12. Gupta B, Revagade N, Hilborn J. Poly (lactic acid) fiber: an overview. Progr Polym Sci 2007;32(4):455-482.

13. Herrera N, Mathew AP, Oksman K. Plasticized polylactic acid/cellulose nanocomposites prepared using melt-extrusion and liquid feeding: mechanical, thermal and optical properties. Compos Sci Technol 2015;106:149-155.

14. Šturcová A, Davies GR, Eichhorn SJ. Elastic Modulus and Stress-Transfer Properties of Tunicate Cellulose Whiskers. Biomacromolecules. 2005;6(2):1055-1061.

15. Fernandes EM, Pires RA, Mano JF, Reis RL. Bionanocomposites from lignocellulosic resources: Properties, applications and future trends for their use in the biomedical field. Progr Polym Sci 2013;38(10):1415-1441.

16. Arrieta MP, Fortunati E, Dominici F, Rayón E, López J, Kenny JM. PLA-PHB/cellulose based films: Mechanical, barrier and disintegration properties. Polym Degrad Stabil 2014;107(0):139-149.

17. Coccia V, Cotana F, Cavalaglio G, Gelosia M, Petrozzi A. Cellulose Nanocrystals Obtained from Cynara Cardunculus and Their Application in the Paper Industry. Sustainability 2014;6(8):5252-5264.

18. Brito BSL, Pereira FV, Putaux J-L, Jean B. Preparation, morphology and structure of cellulose nanocrystals from bamboo fibers. Cellulose 2012;19(5):1527-1536.

19. Fortunati E, Puglia D, Luzi F, Santulli C, Kenny JM, Torre L. Binary PVA bio-nanocomposites containing cellulose nanocrystals extracted from different natural sources: Part I. Carbohyd Polym 2013;97(2):825-836.

20. Neto WPF, Silvério HA, Dantas NO, Pasquini D. Extraction and characterization of cellulose nanocrystals from agro-industrial residue–Soy hulls. Ind Crop Prod 2013;42:480-488.

21 Hsieh Y-L. Cellulose nanocrystals and self-assembled nanostructures from cotton, rice straw and grape skin: a source perspective. J Mater Sci 2013;48(22):7837-7846.

22. Matos Ruiz M, Cavaillé JY, Dufresne A, Gérard JF, Graillat C. Processing and characterization of new thermoset nanocomposites based on cellulose whiskers. Compos Interface 2000;7(2):117-131.

23. Lin N, Dufresne A. Nanocellulose in biomedicine: Current status and future prospect. Eur Polym J 2014;59:302-325.

24. Cranston ED, Gray DG. Morphological and Optical Characterization of Polyelectrolyte Multilayers Incorporating Nanocrystalline Cellulose. Biomacromolecules. 2006;7(9):2522-2530.

25. Silvério HA, Neto WPF, Dantas NO, Pasquini D. Extraction and characterization of cellulose nanocrystals from corncob for application as reinforcing agent in nanocomposites. Ind Crops and Prod 2013;44:427-436.

26. Saïd Azizi Samir MA, Alloin F, Paillet M, Dufresne A. Tangling effect in fibrillated cellulose reinforced nanocomposites. Macromolecules. 2004;37(11):4313-4316.

27. Puglia D, Petrucci R, Fortunati E, Luzi F, Kenny JM, Torre L. Revalorisation of Posidonia Oceanica as Reinforcement in Polyethylene/Maleic Anhydride Grafted Polyethylene Composites. J Renewable Mat 2014;2(1):66-76.

28. Bettaieb F, Khiari R, Hassan ML, Belgacem MN, Bras J, Dufresne A, Mhenni MF, Preparation and characterization of new cellulose nanocrystals from marine biomass Posidonia oceanica. Ind Crop Prod 2015; doi:10.1016/j.indcrop.2014.12.038.

29. Bettaieb F, Khiari R, Dufresne A, Mhenni MF, Putaux JL, Boufi S. Nanofibrillar cellulose from Posidoniaoceanica: Properties and morphological features. Ind Crop Prod 2015; doi:10.1016/j.indcrop.2014.12.060

30. Bettaieb F, Khiari R, Dufresne A, Mhenni MF, Belgacem MN. Mechanical and thermal properties of Posidonia oceanica cellulose nanocrystal reinforced polymer. Carbohyd Polym 2015;123:99-104.

1   31. Khiari R, Marrakchi Z, Belgacem MN, Mauret E, Mhenni F. New lignocellulosic fibres-

2   reinforced composite materials: A stepforward in the valorisation of the Posidonia oceanica balls.

3   Compos Sci Technol 2011;71(16):1867-1872.

4   32. Fortunati E, Luzi F, Puglia D, Petrucci R, Kenny JM, Torre L. Processing of PLA

5   nanocomposites with cellulose nanocrystals extracted from Posidonia oceanica waste: Innovative

6   reuse of coastal plant. Ind Crop Prod 2015;67:439-447.

7   33. Petersson L, Kvien I, Oksman K. Structure and thermal properties of poly (lactic acid)/cellulose

8   whiskers nanocomposite materials. Compos Sci Technol 2007;67(11):2535-2544.

9   34. Liu L, Li S, Garreau H, Vert M. Selective enzymatic degradations of poly (L-lactide) and poly

10   (ε-caprolactone) blend films. Biomacromolecules. 2000;1(3):350-359.

11   35. Li S, Girard A, Garreau H, Vert M. Enzymatic degradation of polylactide stereocopolymers

12   with predominant D-lactyl contents. Polym Degrad Stabil 2000;71(1):61-67.

13   36. Dong J, Liao L, Ma Y, Shi L, Wang G, Fan Z, Li S, Lu Z. Enzyme-catalyzed degradation

14   behavior of l-lactide/trimethylene carbonate/glycolide terpolymers and their composites with poly

15   (l-lactide-co-glycolide) fibers. Polym Degrad Stabil 2014;103:26-34.

16   37. Reeve MS, McCarthy SP, Downey MJ, Gross RA. Polylactide stereochemistry: effect on

17   enzymic degradability. Macromolecules 1994;27(3):825-831.

18   38. MacDonald RT, McCarthy SP, Gross RA. Enzymatic degradability of poly (lactide): effects of

19   chain stereochemistry and material crystallinity. Macromolecules 1996;29(23):7356-7361.

20   39. Heux L, Chauve G, Bonini C. Nonflocculating and chiral-nematic self-ordering of cellulose

21   microcrystals suspensions in nonpolar solvents. Langmuir. 2000;16(21):8210-8212.

22   40. Fortunati E, Armentano I, Zhou Q, Iannoni A, Saino E, Visai L, Berglund LA, Kenny JM.

23   Multifunctional bionanocomposite films of poly(lactic acid), cellulose nanocrystals and silver

24   nanoparticles. Carbohyd Polym 2012;87(2):1596-1605.

25   41. Determination of the degree of disintegration of plastic materials under simulated composting

26   condition in a laboratory-scale test. UN EN ISO 20200 2006.

1   42. Wang C-H, Fan K-R, Hsiue G-H. Enzymatic degradation of PLLA-PEOz-PLLA triblock

2   copolymers. Biomaterials 2005;26(16):2803-2811.

3   43. Turner J, Riga A, O'Connor A, Zhang J, Collis J. Characterization of drawn and undrawn poly-

4   L-lactide films by differential scanning calorimetry. J Therm Anal Calorim 2004;75(1):257-268.

5   44. Kale G, Kijchavengkul T, Auras R, Rubino M, Selke SE, Singh SP. Compostability of

6   bioplastic packaging materials: an overview. Macromol Biosci 2007;7(3):255-277.

7   45. Fortunati E, Luzi F, Puglia D, Dominici F, Santulli C, Kenny JM, Torre L. Investigation of

8   thermo-mechanical, chemical and degradative properties of PLA-limonene films reinforced with

9   cellulose nanocrystals extracted from Phormium tenax leaves. Euro Polym J 2014;56(0):77-91.

10 46. Fukushima K, Abbate C, Tabuani D, Gennari M, Camino G. Biodegradation of poly (lactic

11 acid) and its nanocomposites. Polym Degrad Stabil 2009;94(10):1646-1655.

12 47. Bitinis N, Fortunati E, Verdejo R, Bras J, Maria Kenny J, Torre L, López-Manchado MA.

13 Poly(lactic acid)/natural rubber/cellulose nanocrystal bionanocomposites. Part II: Properties

14 evaluation. Carbohyd Polym 2013;96(2):621-627.

15 48. Paul MA, Delcourt C, Alexandre M, Degée P, Monteverde F, Dubois P.

16 Polylactide/montmorillonite nanocomposites: study of the hydrolytic degradation. Polym Degrad

17 Stabil 2005;87(3):535-542.

18 49. Fortunati E, Peltzer M, Armentano I, Jimenez A, Kenny JM. Combined effects of cellulose

19 nanocrystals and silver nanoparticles on the barrier and migration properties of PLA nano-

20 biocomposites. J Food Eng 2013;118(1):117-124.

21 50. Arrieta MP, López J, Rayón E, Jiménez A. Disintegrability under composting conditions of

22 plasticized PLA–PHB blends. Polym Degrad Stabil 2014; 108: 307-318.

23 51. Arias V, Höglund A, Odelius K, Albertsson AC. Polylactides with "green" plasticizers:

24 Influence of isomer composition. J Appl Polym Sci 2013;130(4):2962-2970.

1 52. Khan A, Khan RA, Salmieri S, Le Tien C, Riedl B, Bouchard J, Chauve G, Tan V, Kamal MR,

2 Lacroix M. Mechanical and barrier properties of nanocrystalline cellulose reinforced chitosan based

3 nanocomposite films. Carbohyd Polym 2012;90(4):1601-1608.

4 53. Sanchez-Garcia MD, Lagaron JM. On the use of plant cellulose nanowhiskers to enhance the

5 barrier properties of polylactic acid. Cellulose 2010;17(5):987-1004.

6 54. Li S, Tenon M, Garreau H, Braud C, Vert M. Enzymatic degradation of stereocopolymers

7 derived from L-, DL-and meso-lactides. Polym Degrad Stabil 2000;67(1):85-90.

8 55. Malwela T, Ray SS. Enzymatic degradation behavior of nanoclay reinforced biodegradable

9 PLA/PBSA blend composites. Int J Biol Macromol 2015;77:131-142.

10 56. Yamashita K, Kikkawa Y, Kurokawa K, Doi Y. Enzymatic degradation of poly (L-lactide) film

11 by proteinase K: quartz crystal microbalance and atomic force microscopy study.

12 Biomacromolecules 2005;6(2):850-857.

13 57. Yasuniwa M, Tsubakihara S, Sugimoto Y, Nakafuku C. Thermal analysis of the

14 double - melting behavior of poly (L - lactic acid). J Polym Sci Pol Phys 2004;42(1):25-32.

15

16

17 **Figure and Table Captions**

18 **Figure 1:** Scheme of CNC extraction process from *Posidonia Oceanica* plant.

19 **Figure 2:** Visual observation (a) and disintegrability values (b) of PLA and PLA nanocomposites

20 before and after different days under composting conditions.

21 **Figure 3:** FESEM investigation of PLA and PLA nanocomposites before and after 3 days in

22 composting conditions.

23 **Figure 4:** Panel A:visual observation (a, b) of PLA and PLA nanocomposites at different times of

24 enzymatic degradation. Panel B: weight loss at different hours (2, 6, 18 and 24 h) (c) and weight

25 loss at different days (d) in enzymatic medium of PLA and PLA nanocomposites. (Different letters

in the graphs c) indicate significant statistical differences among formulations (p<0.05) after 24

hours of test in enzymatic buffer solution).

Figure 5: Water absorption at different hours (2, 6, 18 and 24 h) (b), and water absorption at

different days (c) in enzymatic medium of PLA and PLA nanocomposites. (Different letters in the

graphs c) indicate significant statistical differences among formulations (p<0.05) after 24 hours of

test in enzymatic buffer solution).

Figure 6: FESEM investigation of PLA and PLA nanocomposites after enzymatic degradation.

Figure 7: Derivative curves of weight loss for PLA and PLA nanocomposites at different

enzymatic degradation times.

Figure 8: DSC thermograms at the first heating scan for PLA and PLA nanocomposites. The black

curve is relative to initial time while the red/ lower curve is referred to the final time of incubation

in enzymatic solution for each formulation.

Table 1: Thermal properties of PLA and PLA nanocomposites at different time of enzymatic

degradation at the first heating scan.

1   **Study of disintegrability in compost and enzymatic degradation of PLA and PLA**

2   **nanocomposites reinforced with cellulose nanocrystals extracted from *Posidonia Oceanica***

3

4   F. Luzi, E. Fortunati[*], D. Puglia, R. Petrucci, J.M. Kenny, L. Torre

5

6   University of Perugia, Civil and Environmental Engineering Department, UdR INSTM, Strada di

7   Pentima 4, 05100 Terni (Italy)

8

9   [*]**Corresponding author**: Tel.: +39-0744492921; fax: +39-0744492950; E-mail address:

10   elena.fortunati@unipg.it (E. Fortunati)

11

12   **Abstract**

13   Nanocomposite films based on poly(lactic acid) (PLA) reinforced with cellulose nanocrystals

14   extracted from *Posidonia Oceanica* plant were prepared by solvent casting method containing 1 or

15   3 %wt of cellulose nonocrystals unmodified (CNC) and modified using a commercial surfactant (s-

16   CNC). The modification improves the dispertion of CNC into the matrix. Enzymatic degradation

17   using efficient enzyme proteinase K and disintegrability in composting conditions were considered

18   to gain insights into the post-use degradation processes of the produced formulations. Results of

19   visual, morphological and thermal analysis of enzymatic degradation studies confirmed that the

20   selected enzyme preferentially degraded amorphous regions with respect of crystalline ones, while

21   the crystallinity degree of the nanocomposite films increased during enzymatic degradation, as a

22   consequence of enzyme action. The disintegration in compositing conditions of different

23   formulations was also investigated by means of visual and morphological analysis. The

24   disintegrability in compost conditions showed that the formulations disintegrated in less than 14

25   days, in addition it has been proved that CNC modified with surfactant were able to promote the

26   disintegration behaviour. The production of PLA based nanocomposites incorporating cellulose

27   extract from marine wastes suggested the potential application of the proposed material for short-

28   term food packaging with low enviromental impact.

29

30   **Keywords:** poly(lactic acid), cellulose nanocrystals, *Posidonia Oceanica*, nanocomposites,

31   enzymatic degradation, compost disintegrability.

32

1

1. Introduction

In the last years, biodegradable polymers, that can be decomposed by fungal or microooorganisms, have been considered as promising alternative to petrochemical-based polymers for specific applications [1].

Every year, 140 million tons of petroleum based polymers are produced and introduced in the ecosystem as industrial waste products [2]. Biodegradable polymers are based on renewable materials, such as starch, lignin, cellulose etc., or synthesized from renewable resources. The green materials have a lower negative environmental impact than the petroleum based materials. Poly (lactic acid) (PLA) is one of the most attractive green plastic useful for the production of ecofriendly food packaging [3], it can be degraded into CO_2 and H_2O [4]. It is a linear aliphatic thermoplastic polyester derived from renewable resources such as fermentation of starch and other polysaccharides [5] like corn, rice and sugar beets [6]. PLA is a biocompatible, biodegradable and crystalline polymer, the products manufactured usising this matix completely disintegrated in less than one month in ideal conditions or in specific medium or environments [7]. Moreover, PLA can be processed by injection molding, film extrusion, blow molding, thermoforming, fiber spinning, and film forming and has better thermal processability in comparison with other biopolymers, such as poly (ε-caprolactone)(PCL), poly(hydroxyl alkanoates) (PHAs), etc. [8, 9].

The properties of PLA are dependent on the ratio of D and L enantiomers [10]. It exhibits interesting physical [1] and functional properties as good transparency, good mechanical properties and low cost.

PLA is approved by the Food and Drug Administration (FDA) and can be used in biomedical application, in direct contact with biological fluids and for implantation in the human body and does not produce toxic components [11] or carcinogenic effects in local tissues [8] during the degradation into the body [12]. However, PLA matrix exhibits some limitations when it is used in food applications compared to equivalent traditional polymers, as lower barrier properties

1 (important properties for food packaging), high brittleness, slow crystallization rate and relatively

2 low thermal and mechanical properties [13]. In order to overcome these limitations, several

3 strategies can be adopted to decrease and modulate these properties. The development of

4 nanocomposites or blends represents a valid solution to modify the initial characteristics. The

5 production of nanocomposites reinforced with nanofiller extracted from natural resources is a valid

6 strategy used to increase the physical properties of renewable and biodegradable polymers, without

7 affecting their transparency properties.

8 Cellulose nanocrystals have received, in the last period, a big interest as natural reinforcement able

9 to increase the properties of a biomaterial suitable for food packaging applications [14]. Moreover,

10 CNC present excellent biocompatibility [15], high stiffness and low density [16]. CNC can be

11 extracted from different natural resources as *Cynara Cardunculus* [17], bamboo [18], phormium,

12 flax [19] and other natural sources and waste [20, 21]. The obtained nanostructures are usually

13 characterized by rigid rod monocrystalline domains with diameters ranging from 1-100 nm and

14 from ten to hundreds of nm in length [22]. In general, the nanocrystals aspect ratio

15 (diameter/length) can vary from 1:1 to 1:100 and the dimensions of the CNC depend on the raw

16 material utilized for their extraction [23] and the intensity of the chemical process for their

17 production [24]. CNC have a crystalline structure [25] and an elastic modulus around 150 GPa [26].

18 In this research, CNC extracted from *Posidonia Oceanica* ball wastes have been used. This aquatic

19 plant appears on Mediterranean coastal beaches in big amounts in the form of balls as a consequence

20 of storms that tear off leaves and stems in some cases [27], consequently, the plants have to be

21 removed to maintain the optimum condition of the coastal for the tourists. Several academic

22 research have focused their attention on the revalorization of ligno-cellulosic wastes of *Posidonia*

23 *Oceanica* plant [28-30] as reinforcement or nanoreinforcement in different matrices for bio-based

24 films [31, 32] or as filler for traditional polymer [27].

25 Recently, Fortunati et al. 2015 [32] reported the preparation of CNC extracted from *Posidonia*

26 *Oceanica* balls; in the same research, they also presented the production and the characterization of

3

1 PLA based nanocomposites reinforced with cellulose nanocrystals unmodified (CNC) and modified

2 (s-CNC) with a surfactant.The use of surfactant is a valid strategy to improve the dispersion of the

3 CNC in a polymeric matrix [33]. The positive results obtained by functional, optical and migration

4 properties of PLA based films suggested the possibility of using these bio-based nanocomposites in

5 industrial application.

6 In the present work, enzymatic degradation and disintegrability in composting conditions of PLA

7 nanocomposites reinforced with both unmodified and surfactant modified cellulose nanocrystals

8 extracted from *Posidonia Oceanica* balls have been tested, in order to evaluate the post-use

9 behaviour of these potential food packaging systems. The disintegrability in compost was carried

10 out at 58 °C in aerobic condition and 50 % of humidity.

11 The enzyme selected for the enzymatic degradation test, a protease from *Tritirachium album*,

12 proteinase K, was found to be able to degrade selectively L-lactic bonds and not the D-lactic ones,

13 being poly(D- lactic) not degradable with this specific enzyme [34, 35]. The enzyme shows the

14 major effect on degradation in amorphous region respect to crystalline ones [35-37]. In fact as

15 previously reported in literature the degradation rates of PLA decreased with an increase in

16 crystallinity [38].

17 Visual observation and morphological analysis were performed at different times for each test, with

18 the aim of evaluating how the two different procedures influenced the properties of the films.

19 Moreover, thermal analysis was carried out only for film tested in enzymatic degradation

20 conditions, in order to highlight how proteinase K selectively degraded amorphous regions with

21 respect of crystalline ones.

22

23 **2.Experimental section**

24 **2.1 Materials**

25 Poly(lactic acid) (PLA) in forms of fibres (specific gravity 1.25 g cm^{-3}, 6 mm length), was supplied

26 by MiniFibers, Inc..

1 *Posidonia Oceanica* waste balls were collected from the Campello Beach in Alicante (Spain), by

2 Aitex (Alcoy, Alicante, Spain). *Posidonia Oceanica* is a Mediterranean endemic alga characterized

3 by relatively high amounts of extractives. The preparation of the cellulose nanocrystals (CNC)

4 extracted from *Posidonia Oceanica* was previously described [32]. Briefly, the extraction procedure

5 of cellulose nanocrystals was implemented in two steps (Figure 1). The first step, a chemical alkali

6 treatment, leads to the production of holocellulose by the gradual removal of lignin, while the

7 subsequent sulphuric acid hydrolysis process allows obtaining cellulose nanocrystals in an aqueous

8 suspension from *Posidonia Oceanica* wastes. The mean diameter of the unbleached fibres was

9 84±26 μm, however, after bleaching pre-treatments as a consequence of elimination of lignin,the

10 fibres appeared separated and the mean diameter reduced at about 7±2 μm. The CNC appear

11 individualized and with acicular rod shape, (180 ± 28) nm in length a diameter of (4.9±1.3) with a

12 aspect/ratio of 36.7 [32].

13 Tris(hydroxymethyl)aminomethane/HCl, sodium azide, and proteinase K obtained from

14 *Tritirachium album* (lyophilized powder, ≥ 30 units/mg protein) and all the chemical reagents were

15 supplied by Sigma Aldrich®.

16

17 **2.2 PLA nanocomposite processing**

18 PLA nanocomposite films reinforced with CNC and s-CNC were prepared by solvent casting

19 method using chloroform. Firstly, PLA (0.75 g) was dissolved in 25 mL of $CHCl_3$ with stirring at

20 room temperature (RT). Then specific amount of cellulose nanocrystals (1 wt% and 3 wt% of

21 unmodified (CNC) and modified with commercial surfactant(s-CNC)), were added, and related

22 samples, designed respectively as PLA_1CNC, PLA_3CNC, PLA_1s-CNC and PLA_3s-CNC,

23 were produced. The CNC were modified with a commercial surfactant (Beycostat A B09 - CECCA

24 S.A.) [39], an acid phosphate ester of ethoxylatednonylphenol, with the aim of improving both the

25 dispersion of the nanoreinforcements into the matrix and the final properties of the nanocomposites.

26 The solution of s-CNC was prepared adding the surfactant in the proportion of 1/4 (wt/wt) directly

1 to the CNC aqueous solution. In order to increase the thermal stability of the produced nanocrystals,

2 the pH of CNC and s-CNC aqueous solutions was raised to approximately 9, by using a 0.25 %wt

3 NaOH solution [40].

4 The CNC in powder (unmodified and modified) was added to the $CHCl_3$, forming 1 wt%

5 suspension. The cellulose nanocrystal solution was exposed to sonication (Vibracell, 750W) for 1

6 min in an ice bath.The different solutions were cast onto a 15 cm diameter glass Petri dish and then

7 dried for 24 h at RT.

8

9 **2.3 Disintegrability in composting of PLA and PLA nanocomposites**

10 Disintegrability in composting conditions was carried out following the European standard ISO

11 20200. The test method determines, at laboratory-scale, the degree of disintegration of plastic

12 materials under simulated intensive aerobic composting condition [41]. This method studies the

13 disintegration and not the biodegradability of plastic materials. The degree of disintegration D was

14 calculated in percent by normalizing the sample weight at different days of incubation to the initial

15 weight by using Equation (1):

16 $$D = \frac{m_i - m_r}{m_i} *100$$ (Eq. 1)

17 where:

18 m_i= is the initial dry plastic mass;

19 m_r= is the dry plastic material after the test.

20 PLA and PLA nanocomposite films of dimension 15 mm x 15 mm x 0.03 mm were weighed and

21 buried into the organic substrate at 4-6 cm depth in the perforated boxes guarantying the aerobic

22 conditions and incubated at 58 ºC at 50 % of humidity. The aerobic conditions were guaranteed by

23 mixing periodically the solid soil. The materials tested can be considered disintegrable according to

24 the European standard when 90% of the plastic sample weight shall be lost within 90 days of

25 analysis. In order to simulate the disintegrability in compost, a solid synthetic waste was prepared,

1 mixing sawdust, rabbit food, compost inoculum supplied by Genesu S.p.a., starch, sugar, oil and

2 urea. The water content of the substrate was around 50 % and the aerobic condition was guaranteed

3 into the boxes by hand mixing the materials every day. The different formulations were tested for

4 maximum 14 days. The samples tested were taken out at different times (1, 3, 7, 10 and 14 days),

5 washed with distilled water and dried in a oven at 37 °C for 24 h.

6 The photographs on the samples were taken for visual comparison,while the surface microstructure

7 of the PLA and PLA nanocomposites was investigated, before and after 3 days of incubation, by

8 means of a field emission scanning electron microscope (FESEMSupra 25-Zeiss), after gold

9 sputtering of the samples.

10

11 **2.4 Enzymatic degradation of PLA and PLA nanocomposites**

12 For enzymatic degradation analysis, each sample was cut with dimensions of 15 x 15 x 0.03 mm,

13 and weighed before its immersion in the degradation medium. After that, the samples were placed

14 in vials filled with degradation medium formed by the enzyme (0.5 mg) and 5 mL of

15 tris(hydroxymethyl)aminomethane/HCl buffer (0.05 M, pH 8.6), to optimize the enzyme activity.

16 Sodium azide (0.02 wt %) was added to each buffer solution to inhibit the growth of

17 microorganisms. Enzymatic degradation was performed in an incubator at 37 ºC and the buffer-

18 enzyme system was renewed every 24 hours for 21 days to maintain the enzymatic activity.

19 Specimens (in triplicate) of each formulation were removed for the different time selected for this

20 study. The samples tested were taken out at 2, 6, 18 and 24 hours and at 1, 2, 3, 5, 7, 8, 9, 16 and 21

21 days, washed with distilled water and dried at room temperature up to constant weight.

22 Weight measurements, determined using an analytical balance (± 0.00001 g), and visual

23 observations, were performed for each specimen. The weight loss (WL) of the samples was

24 evaluated by using by using Equation (2):

25 $WL(\%) = \dfrac{(W_0 - W_t)}{W_0} * 100$ (Eq. 2)

1 where:

2 W_0= is the initial dry plastic mass;

3 W_t= is the dry weight of a material after enzymatic degradation.

4 Another important parameter to be considered is the water absorption (WA) during the degradation

5 process, the hydrophilic polymers take up water and the degradation rate increase [42]. It was

6 calculated by using Equation (3):

7 $$WA(\%) = \frac{(W_w - W_t)}{W_t} * 100 \qquad \text{(Eq. 3)}$$

8 where:

9 W_w= is the weight of plastic material after enzymatic degradation;

10 W_t= is the dry weight of a material after enzymatic degradation.

11 Thermal characterization after enzymatic degradation was performed using differential scanning

12 calorimetry (DSC) and thermogravimetric analysis (TGA) at different incubation times.Differential

13 scanning calorimeter (DSC, Mettler Toledo 822/e) investigations were done from -25 to 210°C, at

14 10 °C min^{-1}, applying two heating and one cooling scans in nitrogen atmosphere (50mL min^{-1}).

15 Melting and cold crystallization temperatures and enthalpies (T_m, T_{cc} and ΔH_m, ΔH_{cc}) were

16 determined from the first and second heating scan, while crystallization phenomena were analyzed

17 during the cooling scan. The glass transition temperature (T_g) was registered for each scan. Three

18 samples were used to characterize each formulation.

19 The crystallinity degree was calculated by using Equation (4):

20 $$\chi = \frac{1}{(1 - m_f)} \left[\frac{(\Delta H_m - \Delta H_{cc})}{\Delta H_0} \right] * 100 \qquad \text{(Eq. 4)}$$

21 where ΔH_m is the melt enthalpy and ΔH_{cc} is the cold crystallization enthalpy, ΔH_0 is enthalpy of

22 melting for a 100% crystalline PLA sample, taken as 93 J g^{-1} [43], mf is the weight fraction of

23 nanoreinforcements in the sample and (1-m_f) is the weight fraction of PLA in the sample.

1 Thermogravimetric analysis (TGA - Seiko Exstar 6300) from 30 to 600 °C at 10 °C min^{-1} under a

2 nitrogen atmosphere (250 mL min^{-1}) on 10 mg weight was performed for each sample.

3 Finally, the surface microstructure of the PLA nanocomposites before and after enzymatic

4 degradation at different incubation times was investigated by FESEM.

5

6 **2.5 Statistical analysis**

7 Statistical analysis of data was performed through analysis of variance (ANOVA) using

8 Statgraphics Plus for Windows 5.1 Program (Munugistics Corp., Rockville, MD). Fisher's least

9 significant difference (LSD) was used at the 95% confidence.

10

11 **3. Results and Discussion**

12 **3.1 Disintegrability in composting conditions of PLA and PLA nanocomposites**

13 The disintegrability in composting conditions of PLA and PLA based nanocomposites represents an

14 interesting and attractive property for packaging applications that simulate the post-use of plastics

15 [44, 45]. Composting is a natural process, in which the organic material can be decomposed by

16 microorganisms, including fungi and bacteria. PLA degradation starts with diffusion of water into

17 the materials. The hydrolysis of PLA produces a molecular weight reduction by random non-

18 enzymatic chain scissions of the ester groups, leading to the formation of oligomers and lactic acid.

19 The disintegrability in composting made by microorganisms such as fungi and bacteria starts when

20 the molecular weight of PLA reaches about 10.000-20.000 g mol^{-1}. The microorganisms metabolize

21 the macromolecules as organic matter, converting them to carbon dioxide, water and humus [44].

22 The use of nanoparticles, as nanoreinforcements, influence the biodegradation in compost of PLA

23 and the disintegrability process strongly depends on their hydrophilicity and their nature [46, 47].

24 Figure 2 shows the visual observation (Figure 2,a) and the disintegrability values (Figure 2,b) of the

25 PLA samples reinforced with both unmodified and surfactant modified CNC extracted from

26 *Posidonia Oceanica* taken out at different times of composting. The disintegrability value was

1 evaluated in terms of weight loss as a function of testing time, in which the line at 90 % of

2 disintegration represents the limit point of disintegrability imposed by the ISO 20200; Figure 2,b

3 shows that all the materials reach a degree of disintegration exceeding 90% after 14 days of

4 composting, showing an evident visual fragmentation. After only one day of incubation, the

5 samples start to change their appearance, as it is possible to see in Figure 2,a: the formulations

6 appear white and deformed and this effect is more evident after 3 days in composting conditions.

7 The whitening process and the formulation opacity are attributed to change in the refractive index

8 due to water absorption, with the formation of low molecular weight compounds [47], the creation

9 of some holes on the materials and an induced increase of the crystallinity during degradation [48].

10 Moreover, after 3 days of incubation, PLA_3s-CNC film became breakable respect to the other

11 samples, due to the different morphology of the cross section that characterized this sample, as

12 reported by Fortunati et al 2015 [32]. The cross section of PLA_3s-CNC system, in fact, appears

13 characterized by a porous structure induced by the presence of the surfactant. The presence of the

14 pores favors the process of disintegrability in composting since the internal structure is easily

15 accessible by water and microorganisms. After 7 days of incubation, the films became breakable

16 and the weight loss considerably increases; the PLA_CNC formulations show a reduction in weight

17 of 30-40%, while the PLA_s-CNC based systems show a higher reduction, reaching a 70% of

18 disintegrability for the film reinforced with 3 %wt of cellulose nanocrystals. This different

19 behaviour is correlated to the different morphology of cross sections and to the presence of

20 hydrophilic surfactant in PLA_s-CNC based nanocomposites. The lower disintegration rate

21 obtained for PLA_CNC was attributed to the cellulose nanocrystal introduction that, increasing the

22 crystallinity of the systems, affects the water diffusion through the PLA matrix and, consequently,

23 the disintegration kinetics [45]. The addition of hydrophilic cellulose is expected to accelerate the

24 degradation rate in PLA nanocomposites, but at the same time CNC could also inhibit water

25 diffusion, thus explaining the obtained results [49].

1 Figure 3 shows the FESEM images of the neat PLA and PLA nanocomposites surfaces before and

2 after 3 days in composting conditions. After 3 days at 58 °C, a clear surface erosion with the

3 appearance of holes and porous structures on PLA and all PLA nanocomposites was observed,

4 particularly visible in the PLA_3s-CNC samples [50, 51]. Moreover, the disintegrability experiment

5 took place at 58 °C, temperature higher of the nanocomposite glass transition temperature (T_g)

6 (Table 1 time 0). The higher temperature and the surfactant presence are able to increase the chain

7 mobility [45] facilitating the formation of pores structures on the sample surfaces. The breakable

8 structure facilitates the polymer erosion by microorganisms attack. The erosion surface after 3 days

9 was no so evident for the CNC based systems, confirming the potentiality of the cellulose crystals

10 to induce the crystallization of PLA polymer and to inhibit the diffusion process acting by barrier

11 agents [52, 53].

12

13 **3.2 Enzymatic degradation of PLA and PLA nanocomposites**

14 Figure 4 shows the images of different films (Figure 4,a,b- Panel A) and weigh loss curves (Figure

15 4,a-b - Panel B) of the studied samples as a function of different degradation times. After 6 hours of

16 incubation, the samples start to change, as it is possible to see by visual observation (Figure 4,a); the

17 transparency clearly decreases and all the formulations appear opaque, white and deformed. After

18 24 hours in the medium, PLA and PLA nanocomposites show a linear increase of the weight loss. It

19 was observed a higher degradation for PLA neat films with respect to PLA nanocomposites. After

20 only 24 hours of incubation, the PLA showed up to (88.3±1.4) % of weight loss. These results

21 confirm that PLA degradation is catalysed by proteinase K [35, 54]. On the other hand, PLA and

22 PLA reinforced with CNC appeared degraded after 6 hours of test reaching 40-60 % of degradation

23 while PLA reinforced with s-CNC maintained the weight loss lower to 10 % (Figure 4 a, Panel B).

24 Specifically, the weight loss of neat PLA is (88.3±1.4)% after 24 h, followed by PLA_1CNC

25 (69.0±0.9) %, PLA_3CNC (63.2±3.7) %, while the weight loss is (16.6±1.3) % and (23.1±2.3) %,

26 for PLA_1-s-CNC and PLA_3-s-CNC, respectively.

1   The different behaviour that characterizes the CNC and s-CNC based formulations can be attributed

2   to the presence of surfactant. In detail, we notice that the surfactant, an acid phosphate ester of

3   ethoxylatednonyl phenol, is able to decrease the pH level of the aqueous solution (pH = 4-5)

4   inhibiting the action of the enzyme that needs a pH ranged from 7.5 to 12 to explain its action [35,

5   41, 55].

6   Figure 5 shows the water absorption during the first 24 hours (Figure 5, a) till to 21 days (Figure 5,

7   b). All the formulations reach the saturation limit of water absorption after 18 hours in contact with

8   the enzyme containing solution. The formulations reinforced with s-CNC show higher water

9   absorption values; this behaviour can be related to the presence of micro-holes, basically due to the

10   presence of the hydrophilic surfactant used to improve the dispersion of CNC into the matrix, as

11   previously reported [32].

12   FESEM images of the samples, at different incubation times during enzymatic degradation, are

13   reported in Figure 6. After 2 hours, a change in the system morphologies was observed. A clear

14   surface erosion with several and tiny holes and channels on PLA and PLA_CNC surfaces are

15   observed. A similar result about morphological investigation was previously obtained by Malwela

16   et Ray (2015) in the enzymatic degradation study of PLA/PBSA blend composites [55]. The surface

17   modification and the presence of holes and the porous structures can be due to the degradation of

18   the amorphous region eroded preferentially by proteinase K [35, 56]. This effect is not so evident in

19   the case of PLA_s-CNC based formulations, that maintain their original topography till 24 h of

20   incubation with the enzyme. A more evident surface erosion for PLA_s-CNC based formulations is

21   visible after 3 and 7 days in contact with the enzyme containing solution in accord with the slower

22   degradation kinetic detected by the weight loss measurements previously discuss.

23

24   **3.2.1 Thermal properties of PLA nanocomposites after enzymatic degradation**

25   The thermal properties of PLA and PLA nanocomposites at different incubation times are

26   investigated by TGA and DSC. The derivative curves of the mass loss (DTG) for the different

1 studied formulations are reported in Figure 7, while the DSC thermal properties are summarized in

2 Table 1 and Figure 8 (first heating scans for all the materials).

3 Thermogravimetric analysis (Figure 7) of PLA revealed a reduction of the main peak temperature

4 (temperature of maximum degradation rate) that shifts of about 20 °C to lower temperature, after

5 only 2 hours in contact with the enzyme (Figure 7, a). Moreover, the PLA maximum degradation

6 temperature shifts from 332 °C to 278 °C after 2 days of incubation (2 days represent the last time

7 for PLA enzymatic degradation). A different behaviour is detected for PLA reinforced with

8 unmodified and modified cellulose nanocrystals. The main degradation temperature of PLA_1CNC

9 and PLA_3CNC during the enzymatic degradation remains unmodified as previously observed in

10 literature proving that CNC are able to improve the thermal stability of the PLA matrix (Figure 7,

11 b,c) [44, 54]. PLA_1s-CNC and PLA_3s-CNC curves (Figure 7, d,e) show two main peaks of

12 degradation: the first one is associated to the PLA degradation around 330 °C while the second one,

13 at around 500 °C, is related to the surfactant degradation [40]. The variation of the main

14 degradation peaks becomes relevant when the surfactant starts to be released from the formulations

15 and the evidence of the surfactant release from the s-CNC based films is clearly detected in the

16 insert of Figure 7, e. When the surfactant weight starts to decrease (reduction in the intensity of the

17 peak at around 500 °C), also the maximum degradation peak starts to shift to lower temperature as

18 evidence of the occurring degradation mechanism. In particular, the weight loss of PLA_1s-CNC

19 formulation increases after 8 days in enzymatic medium and the same phenomenon is detected for

20 PLA_3s-CNC after 2 days of incubation. As just discussed above, the presence of surfactant in the

21 PLA nanocomposites improves the dispersion of CNC but at same time obstacles the enzyme

22 activity modifying the pH of the medium [42]. Moreover, a higher degradation kinetics of PLA_3s-

23 CNC with respect to the PLA_1s-CNC is observed. The degradation of PLA_3s-CNC is accelerated

24 by the presence of several holes on the fractured surface [32] that facilitated the hydrolytic

25 degradation of the PLA. In particular, the main peak for PLA_1-s-CNC, shifts from 330 °C to 302

26 °C after 21 days while PLA_3-s-CNC reaches 304 °C after only 5 days.

Figure 8 shows the DSC thermograms related to the first heating scan, underlining the variation of crystallization and melting properties at the beginning and at the end of the enzymatic degradation test. The DSC experiments are performed with the aim of investigating the thermal behaviour of PLA nanocomposites during the enzymatic degradation. As it is possible to observe, for PLA and PLA_CNC systems the peak of the cold crystallization disappears completely at the end of test, while for PLA_s-CNC based nanocomposites the peak decreases in its intensity. The melting peak of nanocomposites at initial time is characterized by the presence of two melting peaks. The first peak disappears during the degradation test as observed by thermograms and as reported in Table 1. During the first heating scan (Table 1) some changes are observed in glass transition temperature, cold crystallization temperature, melting enthalpy and cold crystallization enthalpy while for the second value of melting temperature not significant changes are detected. The cold crystallization enthalpy decreases, while the melting enthalpy increases with the time encouraging the crystallization according with literature [42]. The crystallinity degree values, calculated at time zero, are (8.9±3.4), (8.6±3.0), (7.5±1.7), (9.5±0.2) and (11.4±2.0) respectively for PLA, PLA_1CNC, PLA_3CNC, PLA_1s-CNC and PLA_3s-CNC. The same values, calculated at the final stage of the enzymatic degradation for each formulations, increased up to (35.4±0.8), (31.9±0.9), (24.5±0.7), (35.1±3.7) and (31.1±0.5) respectively for PLA, PLA_1CNC, PLA_3CNC, PLA_1s-CNC and PLA_3s-CNC. The increase in crystallinity degree highlights the action of specific enzyme able to degrade amorphous regions [35]. The increase in crystallinity degree can be correlated to the visual appearance of the sample surfaces of PLA and PLA nanocomposites: the films change the colour becoming white, opaque and deformed. Moreover, the two melting peaks of neat PLA, PLA_1CNC PLA_3CNC are associated to the coexistence of two kinds of crystalline structure of PLA [57], while this effect is not evident in the case of PLA reinforced with s-CNC.

4. Conclusions

This research involved two different studies for simulation, at laboratory scale, of the post use of nanocomposite films based on poly(lactic acid) (PLA) and cellulose nanocrystals (CNC) extracted from *Posidonia Oceanica* plant prepared by solvent casting method. The films disintegrated completely during 14 days of the test. The disintegration rate in composting condition was increased by the presence of s-CNC, due to the hydrophilicity of the surfactant. In particular, the disintegrability of PLA_3s-CNC is accelerated by the presence of holes detected by morphology study on cross section surfaces.

Proteinase K strongly catalysed the degradation of PLA and PLA nanocomposites, this effect was delayed in PLA_s-CNC based nanocomposites. This behaviour can be related to the presence of surfactant that, in enzymatic buffer, can be released changing the optimum conditions for the enzyme activity. In fact, it was observed that the degradation values in enzyme buffer for PLA_s-CNC increased with decreased presence of surfactant, as detected by thermogravimetric analysis. PLA and PLA_CNC films degraded completely in two days in enzymatic medium. Moreover, proteinase K degraded preferentially the amorphous region with respect of crystalline one. The DSC analysis confirmed the higher value of crystallinity degrees obtained during the different degradation times.

References

1. Stloukal P, Kalendová A, Mattausch H, Laske S, Holzer C, Koutny M. The influence of a hydrolysis-inhibiting additive on the degradation and biodegradation of PLA and its nanocomposites. Polym Test 2015;41:124-132.

2. Madhavan Nampoothiri K, Nair NR, John RP. An overview of the recent developments in polylactide (PLA) research. Bioresource Technol 2010;101(22):8493-8501.

3. Averous L. Biodegradable multiphase systems based on plasticized starch: A review. J Macromol Sci Polym R 2004;C44(3):231-274.

4. Arjmandi R, Hassan A, Eichhorn SJ, Haafiz MKM, Zakaria Z, Tanjung FA. Enhanced ductility and tensile properties of hybrid montmorillonite/cellulose nanowhiskers reinforced polylactic acid nanocomposites. J Mater Sci 2015;50(8):3118-3130.

5. Arrieta MP, Samper MD, López J, Jiménez A. Combined Effect of Poly (hydroxybutyrate) and Plasticizers on Polylactic acid Properties for Film Intended for Food Packaging. J Polym Environment 2014;22(2):460-470.

6. Dong Y, Ghataura A, Takagi H, Haroosh HJ, Nakagaito AN, Lau K-T. Polylactic acid (PLA) biocomposites reinforced with coir fibres: Evaluation of mechanical performance and multifunctional properties. Compos Part A-Appl S 2014;63:76-84.

7. Jonoobi M, Harun J, Mathew AP, Oksman K. Mechanical properties of cellulose nanofiber (CNF) reinforced polylactic acid (PLA) prepared by twin screw extrusion. Compos Sci Technol 2010;70(12):1742-1747.

8. Rasal RM, Janorkar AV, Hirt DE. Poly (lactic acid) modifications. Prog Polym Sci 2010;35(3):338-356.

9. Arrieta MP, López J, Hernández A, Rayón E. Ternary PLA–PHB–Limonene blends intended for biodegradable food packaging applications. Eur Polym J 2014;50(0):255-270.

10. Abdelwahab MA, Flynn A, Chiou B-S, Imam S, Orts W, Chiellini E. Thermal, mechanical and morphological characterization of plasticized PLA–PHB blends. Polym Degrad Stabil 2012;97(9):1822-1828.

11. Armentano I, Bitinis N, Fortunati E, Mattioli S, Rescignano N, Verdejo R, Lopez-Manchado MA, Kenny JM. Multifunctional nanostructured PLA materials for packaging and tissue engineering. Progr Polym Sci 2013;38(10):1720-1747.

12. Gupta B, Revagade N, Hilborn J. Poly (lactic acid) fiber: an overview. Progr Polym Sci 2007;32(4):455-482.

13. Herrera N, Mathew AP, Oksman K. Plasticized polylactic acid/cellulose nanocomposites prepared using melt-extrusion and liquid feeding: mechanical, thermal and optical properties. Compos Sci Technol 2015;106:149-155.

14. Šturcová A, Davies GR, Eichhorn SJ. Elastic Modulus and Stress-Transfer Properties of Tunicate Cellulose Whiskers. Biomacromolecules. 2005;6(2):1055-1061.

15. Fernandes EM, Pires RA, Mano JF, Reis RL. Bionanocomposites from lignocellulosic resources: Properties, applications and future trends for their use in the biomedical field. Progr Polym Sci 2013;38(10):1415-1441.

16. Arrieta MP, Fortunati E, Dominici F, Rayón E, López J, Kenny JM. PLA-PHB/cellulose based films: Mechanical, barrier and disintegration properties. Polym Degrad Stabil 2014;107(0):139-149.

17. Coccia V, Cotana F, Cavalaglio G, Gelosia M, Petrozzi A. Cellulose Nanocrystals Obtained from Cynara Cardunculus and Their Application in the Paper Industry. Sustainability 2014;6(8):5252-5264.

18. Brito BSL, Pereira FV, Putaux J-L, Jean B. Preparation, morphology and structure of cellulose nanocrystals from bamboo fibers. Cellulose 2012;19(5):1527-1536.

19. Fortunati E, Puglia D, Luzi F, Santulli C, Kenny JM, Torre L. Binary PVA bio-nanocomposites containing cellulose nanocrystals extracted from different natural sources: Part I. Carbohyd Polym 2013;97(2):825-836.

20. Neto WPF, Silvério HA, Dantas NO, Pasquini D. Extraction and characterization of cellulose nanocrystals from agro-industrial residue–Soy hulls. Ind Crop Prod 2013;42:480-488.

21 Hsieh Y-L. Cellulose nanocrystals and self-assembled nanostructures from cotton, rice straw and grape skin: a source perspective. J Mater Sci 2013;48(22):7837-7846.

22. Matos Ruiz M, Cavaillé JY, Dufresne A, Gérard JF, Graillat C. Processing and characterization of new thermoset nanocomposites based on cellulose whiskers. Compos Interface 2000;7(2):117-131.

23. Lin N, Dufresne A. Nanocellulose in biomedicine: Current status and future prospect. Eur Polym J 2014;59:302-325.

24. Cranston ED, Gray DG. Morphological and Optical Characterization of Polyelectrolyte Multilayers Incorporating Nanocrystalline Cellulose. Biomacromolecules. 2006;7(9):2522-2530.

25. Silvério HA, Neto WPF, Dantas NO, Pasquini D. Extraction and characterization of cellulose nanocrystals from corncob for application as reinforcing agent in nanocomposites. Ind Crops and Prod 2013;44:427-436.

26. Saïd Azizi Samir MA, Alloin F, Paillet M, Dufresne A. Tangling effect in fibrillated cellulose reinforced nanocomposites. Macromolecules. 2004;37(11):4313-4316.

27. Puglia D, Petrucci R, Fortunati E, Luzi F, Kenny JM, Torre L. Revalorisation of Posidonia Oceanica as Reinforcement in Polyethylene/Maleic Anhydride Grafted Polyethylene Composites. J Renewable Mat 2014;2(1):66-76.

28. Bettaieb F, Khiari R, Hassan ML, Belgacem MN, Bras J, Dufresne A, Mhenni MF, Preparation and characterization of new cellulose nanocrystals from marine biomass Posidonia oceanica. Ind Crop Prod 2015; doi:10.1016/j.indcrop.2014.12.038.

29. Bettaieb F, Khiari R, Dufresne A, Mhenni MF, Putaux JL, Boufi S. Nanofibrillar cellulose from Posidoniaoceanica: Properties and morphological features. Ind Crop Prod 2015; doi:10.1016/j.indcrop.2014.12.060

30. Bettaieb F, Khiari R, Dufresne A, Mhenni MF, Belgacem MN. Mechanical and thermal properties of Posidonia oceanica cellulose nanocrystal reinforced polymer. Carbohyd Polym 2015;123:99-104.

1   31. Khiari R, Marrakchi Z, Belgacem MN, Mauret E, Mhenni F. New lignocellulosic fibres-

2   reinforced composite materials: A stepforward in the valorisation of the Posidonia oceanica balls.

3   Compos Sci Technol 2011;71(16):1867-1872.

4   32. Fortunati E, Luzi F, Puglia D, Petrucci R, Kenny JM, Torre L. Processing of PLA

5   nanocomposites with cellulose nanocrystals extracted from Posidonia oceanica waste: Innovative

6   reuse of coastal plant. Ind Crop Prod 2015;67:439-447.

7   33. Petersson L, Kvien I, Oksman K. Structure and thermal properties of poly (lactic acid)/cellulose

8   whiskers nanocomposite materials. Compos Sci Technol 2007;67(11):2535-2544.

9   34. Liu L, Li S, Garreau H, Vert M. Selective enzymatic degradations of poly (L-lactide) and poly

10 (ε-caprolactone) blend films. Biomacromolecules. 2000;1(3):350-359.

11 35. Li S, Girard A, Garreau H, Vert M. Enzymatic degradation of polylactide stereocopolymers

12 with predominant D-lactyl contents. Polym Degrad Stabil 2000;71(1):61-67.

13 36. Dong J, Liao L, Ma Y, Shi L, Wang G, Fan Z, Li S, Lu Z. Enzyme-catalyzed degradation

14 behavior of l-lactide/trimethylene carbonate/glycolide terpolymers and their composites with poly

15 (l-lactide-co-glycolide) fibers. Polym Degrad Stabil 2014;103:26-34.

16 37. Reeve MS, McCarthy SP, Downey MJ, Gross RA. Polylactide stereochemistry: effect on

17 enzymic degradability. Macromolecules 1994;27(3):825-831.

18 38. MacDonald RT, McCarthy SP, Gross RA. Enzymatic degradability of poly (lactide): effects of

19 chain stereochemistry and material crystallinity. Macromolecules 1996;29(23):7356-7361.

20 39. Heux L, Chauve G, Bonini C. Nonflocculating and chiral-nematic self-ordering of cellulose

21 microcrystals suspensions in nonpolar solvents. Langmuir. 2000;16(21):8210-8212.

22 40. Fortunati E, Armentano I, Zhou Q, Iannoni A, Saino E, Visai L, Berglund LA, Kenny JM.

23 Multifunctional bionanocomposite films of poly(lactic acid), cellulose nanocrystals and silver

24 nanoparticles. Carbohyd Polym 2012;87(2):1596-1605.

25 41. Determination of the degree of disintegration of plastic materials under simulated composting

26 condition in a laboratory-scale test. UN EN ISO 20200 2006.

42. Wang C-H, Fan K-R, Hsiue G-H. Enzymatic degradation of PLLA-PEOz-PLLA triblock copolymers. Biomaterials 2005;26(16):2803-2811.

43. Turner J, Riga A, O'Connor A, Zhang J, Collis J. Characterization of drawn and undrawn poly-L-lactide films by differential scanning calorimetry. J Therm Anal Calorim 2004;75(1):257-268.

44. Kale G, Kijchavengkul T, Auras R, Rubino M, Selke SE, Singh SP. Compostability of bioplastic packaging materials: an overview. Macromol Biosci 2007;7(3):255-277.

45. Fortunati E, Luzi F, Puglia D, Dominici F, Santulli C, Kenny JM, Torre L. Investigation of thermo-mechanical, chemical and degradative properties of PLA-limonene films reinforced with cellulose nanocrystals extracted from Phormium tenax leaves. Euro Polym J 2014;56(0):77-91.

46. Fukushima K, Abbate C, Tabuani D, Gennari M, Camino G. Biodegradation of poly (lactic acid) and its nanocomposites. Polym Degrad Stabil 2009;94(10):1646-1655.

47. Bitinis N, Fortunati E, Verdejo R, Bras J, Maria Kenny J, Torre L, López-Manchado MA. Poly(lactic acid)/natural rubber/cellulose nanocrystal bionanocomposites. Part II: Properties evaluation. Carbohyd Polym 2013;96(2):621-627.

48. Paul MA, Delcourt C, Alexandre M, Degée P, Monteverde F, Dubois P. Polylactide/montmorillonite nanocomposites: study of the hydrolytic degradation. Polym Degrad Stabil 2005;87(3):535-542.

49. Fortunati E, Peltzer M, Armentano I, Jimenez A, Kenny JM. Combined effects of cellulose nanocrystals and silver nanoparticles on the barrier and migration properties of PLA nano-biocomposites. J Food Eng 2013;118(1):117-124.

50. Arrieta MP, López J, Rayón E, Jiménez A. Disintegrability under composting conditions of plasticized PLA–PHB blends. Polym Degrad Stabil 2014; 108: 307-318.

51. Arias V, Höglund A, Odelius K, Albertsson AC. Polylactides with "green" plasticizers: Influence of isomer composition. J Appl Polym Sci 2013;130(4):2962-2970.

1 52. Khan A, Khan RA, Salmieri S, Le Tien C, Riedl B, Bouchard J, Chauve G, Tan V, Kamal MR,

2 Lacroix M. Mechanical and barrier properties of nanocrystalline cellulose reinforced chitosan based

3 nanocomposite films. Carbohyd Polym 2012;90(4):1601-1608.

4 53. Sanchez-Garcia MD, Lagaron JM. On the use of plant cellulose nanowhiskers to enhance the

5 barrier properties of polylactic acid. Cellulose 2010;17(5):987-1004.

6 54. Li S, Tenon M, Garreau H, Braud C, Vert M. Enzymatic degradation of stereocopolymers

7 derived from L-, DL-and meso-lactides. Polym Degrad Stabil 2000;67(1):85-90.

8 55. Malwela T, Ray SS. Enzymatic degradation behavior of nanoclay reinforced biodegradable

9 PLA/PBSA blend composites. Int J Biol Macromol 2015;77:131-142.

10 56. Yamashita K, Kikkawa Y, Kurokawa K, Doi Y. Enzymatic degradation of poly (L-lactide) film

11 by proteinase K: quartz crystal microbalance and atomic force microscopy study.

12 Biomacromolecules 2005;6(2):850-857.

13 57. Yasuniwa M, Tsubakihara S, Sugimoto Y, Nakafuku C. Thermal analysis of the

14 double‐melting behavior of poly (L‐lactic acid). J Polym Sci Pol Phys 2004;42(1):25-32.

15

16

17 **Figure and Table Captions**

18 **Figure 1:** Scheme of CNC extraction process from *Posidonia Oceanica* plant.

19 **Figure 2:** Visual observation (a) and disintegrability values (b) of PLA and PLA nanocomposites

20 before and after different days under composting conditions.

21 **Figure 3:** FESEM investigation of PLA and PLA nanocomposites before and after 3 days in

22 composting conditions.

23 **Figure 4:** Panel A:visual observation (a, b) of PLA and PLA nanocomposites at different times of

24 enzymatic degradation. Panel B: weight loss at different hours (2, 6, 18 and 24 h) (c) and weight

25 loss at different days (d) in enzymatic medium of PLA and PLA nanocomposites. (Different letters

1   in the graphs c) indicate significant statistical differences among formulations (p<0.05) after 24

2   hours of test in enzymatic buffer solution).

3   **Figure 5:** Water absorption at different hours (2, 6, 18 and 24 h) (b), and water absorption at

4   different days (c) in enzymatic medium of PLA and PLA nanocomposites. (Different letters in the

5   graphs c) indicate significant statistical differences among formulations (p<0.05) after 24 hours of

6   test in enzymatic buffer solution).

7   **Figure 6:** FESEM investigation of PLA and PLA nanocomposites after enzymatic degradation.

8   **Figure 7:** Derivative curves of weight loss for PLA and PLA nanocomposites at different

9   enzymatic degradation times.

10   **Figure 8:** DSC thermograms at the first heating scan for PLA and PLA nanocomposites. The black

11   curve is relative to initial time while the red/ lower curve is referred to the final time of incubation

12   in enzymatic solution for each formulation.

13

14   **Table 1:** Thermal properties of PLA and PLA nanocomposites at different time of enzymatic

15   degradation at the first heating scan.

16

17

Table 1

Formulations	Time	First heating				,	,,	
		T_g(°C)	ΔH_{cc}(J/g)	T_{cc}(°C)	ΔH_m(J/g)	T_m(°C)	T_m(°C)	X_c
PLA	0 h	32.5±2.4[a]	20.5±2.8[c]	83.4±3.4[a]	28.8±1.1[a]	157.0±1.2	166.1±0.7[b]	8.9±3.4[a]
	2 h	39.1±0.5[b]	16.0±0.3[b]	80.0±0.7[a]	31.9±0.5[bc]	-	165.7±0.7[b]	17.1±0.3[b]
	6 h	50.2±0.5[c]	13.0±0.6[b]	89.9±0.8[b]	35.2±0.7[d]	-	160.9±0.9[a]	21.8±0.2[b]
	18 h	53.8±0.6[d]	2.7±0.3[a]	90.9±2.2[b]	29.9±0.3[ab]	-	162.2±0.4[a]	29.9±0.3[c]
	24 h	55.6±0.4[d]	1.3±0.2[a]	128.6±0.1[c]	31.5±1.3[bc]	-	165.0±0.5[b]	32.5±1.7[cd]
	2 d	58.0±1.0[e]	-	-	33.0±0.8[cd]	-	166.2±0.8[b]	35.4±0.8[d]
PLA_1CNC	0 h	35.7±2.2[a]	21.6±3.6[c]	85.0±1.0[a]	29.6±2.9[a]	156.6±1.1[a]	163.5±3.0[a]	8.6±3.0[a]
	2 h	41.1±0.6[b]	13.9±1.2[b]	84.0±0.7[a]	32.0±0.7[a]	155.8±0.6[a]	166.2±0.8[a]	19.2±2.1[b]
	6 h	49.1±2.0[c]	13.0±0.3[b]	88.9±0.8[b]	33.0±0.6[a]	-	165.9±0.9[a]	21.3±1.0[b]
	18 h	55.0±0.7[d]	2.3±0.2[a]	90.9±0.8[b]	29.7±1.6[a]	-	166.1±1.1[a]	29.1±1.5[c]
	24 h	60.0±0.5[e]	2.5±0.1[a]	90.3±0.2[b]	30.7±0.2[a]	-	163.3±0.8[a]	30.1±0.2[c]
	2 d	59.3±0.9[e]	-	-	29.9±0.8[a]	-	165.2±0.8[a]	31.9±0.9[c]
PLA_3CNC	0 h	36.6±1.8[a]	22.1±3.0[c]	84.9±0.1[b]	29.2±1.3[b]	145.4±0.6[a]	157.9±0.1[a]	7.5±1.7[a]
	2 h	38.2±1.0[a]	13.8±1.0[b]	80.1±0.6[a]	30.8±0.4[b]	155.8±0.6[b]	166.1±0.5[b]	17.7±1.4[b]
	6 h	44.5±1.5[b]	11.2±1.0[b]	80.8±1.0[a]	30.8±1.1[b]	-	164.9±0.6[b]	20.4±0.1[b]
	18 h	43.3±3.1[b]	5.6±0.7[a]	87.6±0.7[bc]	29.2±1.0[b]	-	166.0±1.1[b]	20.4±0.1[c]
	24 h	59.0±0.8[c]	2.7±0.2[a]	88.9±2.0[c]	26.1±0.9[a]	-	165.7±1.0[b]	24.5±0.7[c]
PLA_1s-CNC	0h	36.7±0.7[a]	21.8±2.8[e]	79.5±0.7[abc]	30.8±2.6[a]	-	159.9±2.8[a]	9.5±0.2[a]
	2h	52.7±0.6[b]	14.8±0.9[d]	74.8±1.0[a]	30.8±0.4[a]	-	165.3±0.7[b]	17.0±1.4[b]
	6h	52.8±1.9[b]	14.9±0.5[d]	76.1±0.5[ab]	32.7±0.7[ab]	-	165.0±0.2[b]	19.0±1.3[b]
	18h	52.2±0.2[b]	15.0±0.6[d]	76.2±1.1[ab]	33.8±2.4[ab]	-	164.0±0.7[b]	20.1±3.2[b]
	24h	55.0±0.4[cde]	10.7±0.7[c]	77.9±2.0[ab]	34.6±0.5[ab]	-	162.9±0.9[b]	25.5±0.3[c]
	2 d	56.5±1.5[ef]	5.4±0.1[b]	80.7±0.7[bc]	33.5±1.6[ab]	-	164.2±0.4[b]	29.9±1.7[d]
	3 d	54.1±0.8[bcd]	5.5±0.1[b]	87.0±2.3	34.5±1.8[ab]	-	164.8±0.4[b]	30.9±1.8[d]
	5 d	54.8±0.6[bc]	5.2±0.1[b]	80.5±5.5[bc]	35.4±1.2[b]	-	163.2±1.0[b]	32.2±1.4[de]
	7 d	55.2±0.7[de]	4.2±0.1[b]	84.7±1.6[de]	35.2±2.5[b]	-	163.4±1.3[b]	33.0±2.7[d]
	8 d	55.7±0.7[de]	1.5±0.5[a]	90.4±2.7[e]	34.1±1.3[ab]	-	163.8±0.8[b]	34.7±0.9[ef]
	9 d	59.4±1.7[gh]	-	-	34.5±1.4[ab]	-	163.8±0.8[b]	36.7±1.5[f]
	16 d	60.2±0.4[h]	-	-	34.3±1.2[ab]	-	164.0±1.2[b]	36.6±1.3[f]
	21 d	59.1±0.6[fg]	-	-	33.0±3.5[ab]	-	163.2±1.1[b]	35.1±3.7[f]
PLA_3s-CNC	0h	39.2±1.9[a]	21.3±1.3[e]	82.6±0.6[bc]	32.2±1.3[a]	-	161.8±1.3[a]	11.4±2.0[a]
	2h	40.3±0.3[a]	18.3±0.4[d]	77.3±4.1[a]	32.6±0.5[a]	-	164.2±0.9[cd]	15.0±0.2[b]
	6h	53.4±2.2[b]	16.9±2.0[cd]	79.7±1.2[ab]	31.5±1.4[a]	-	164.7±0.6[d]	15.2±0.6[b]
	18h	56.7±0.3[bc]	17.9±0.5[d]	81.9±0.8[bc]	36.7±0.2[c]	-	163.2±0.1[bcd]	19.6±0.3[c]
	24h	54.8±0.4[b]	15.6±0.1[c]	81.9±0.8[bc]	34.6±0.7[b]	-	162.7±1.7[abc]	19.8±0.6[c]
	2 d	56.4±0.3[bc]	13.3±0.2[b]	83.0±0.5[c]	37.3±0.2[c]	-	163.5±0.1[bcd]	25.1±0.5[d]
	3 d	52.8±0.9[bc]	13.2±0.1[b]	82.1±0.1[bc]	37.0±0.7[c]	-	163.5±0.1[bcd]	24.8±0.7[d]
	5 d	52.7±0.7[bc]	8.3±0.1[a]	76.7±1.5[a]	36.6±0.3[c]	-	162.9±0.6[ab]	29.6±0.4[e]
	7 d	55.3±0.1[c]	7.8±0.4[a]	81.8±0.7[bc]	36.1±0.9[c]	-	162.9±0.6[abc]	29.6±0.5[e]
	8 d	55.3±0.7[c]	7.3±0.2[a]	82.1±0.6[bc]	37.4±0.2[c]	-	164.0±0.7[bcd]	31.3±0.5[f]

different letter in the same column indicate significant differences among formulations (p<0.05).

Figure 1

Original lignocellulosic materials

Chemical pretreatment

Acid Hydrolysis

CNC

100 μm

100 μm

1 μm

Figure 2
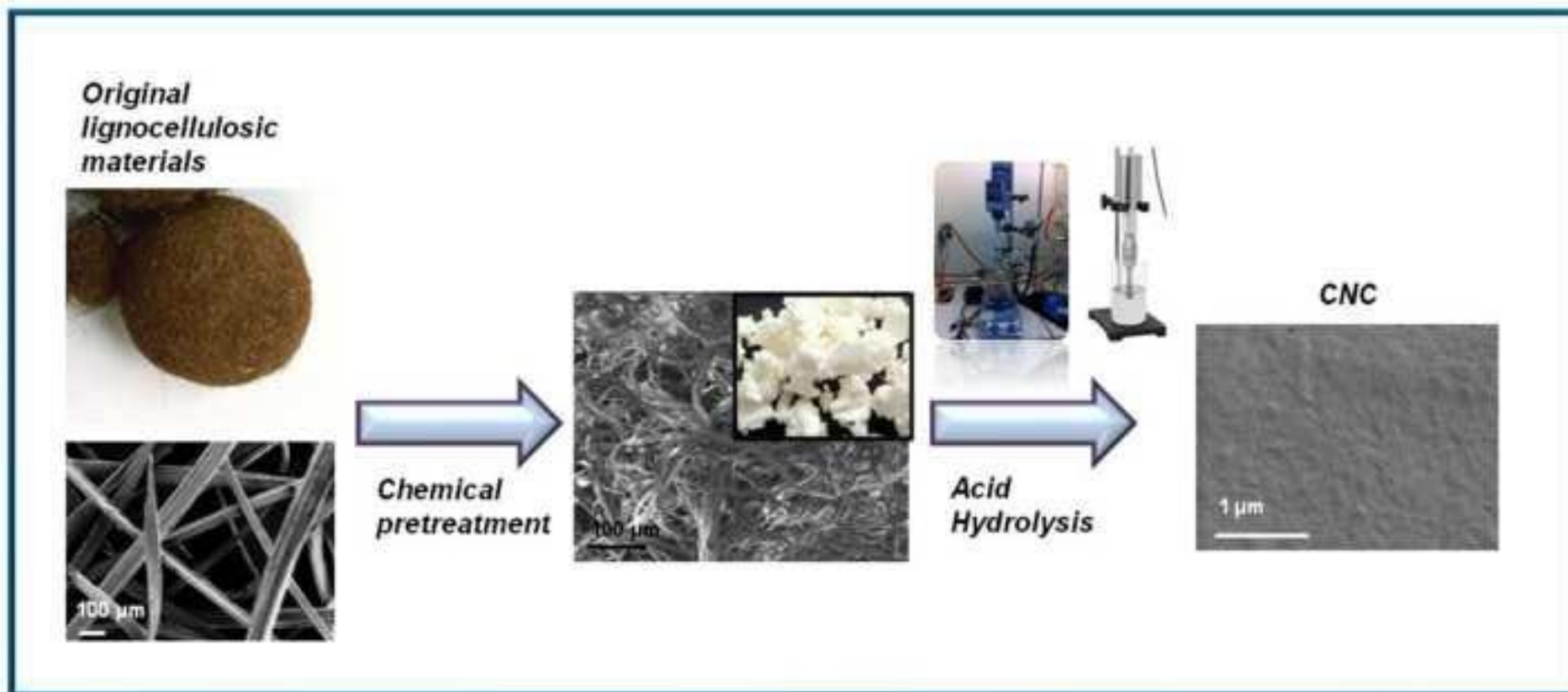**Click here to download high resolution image**

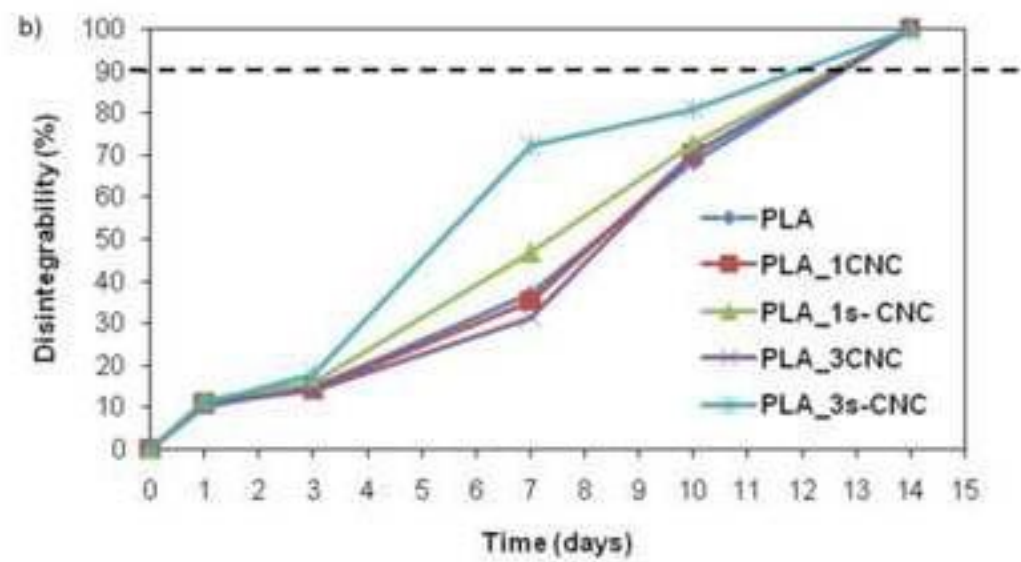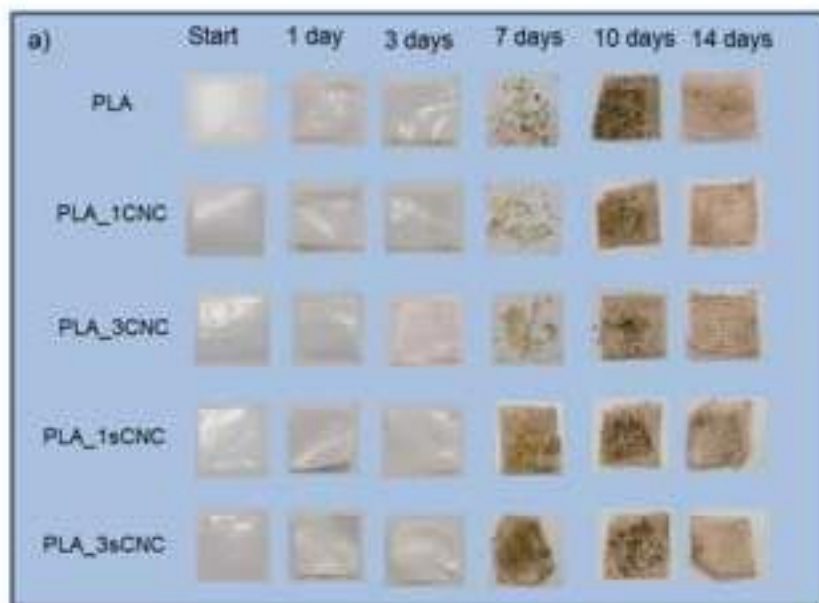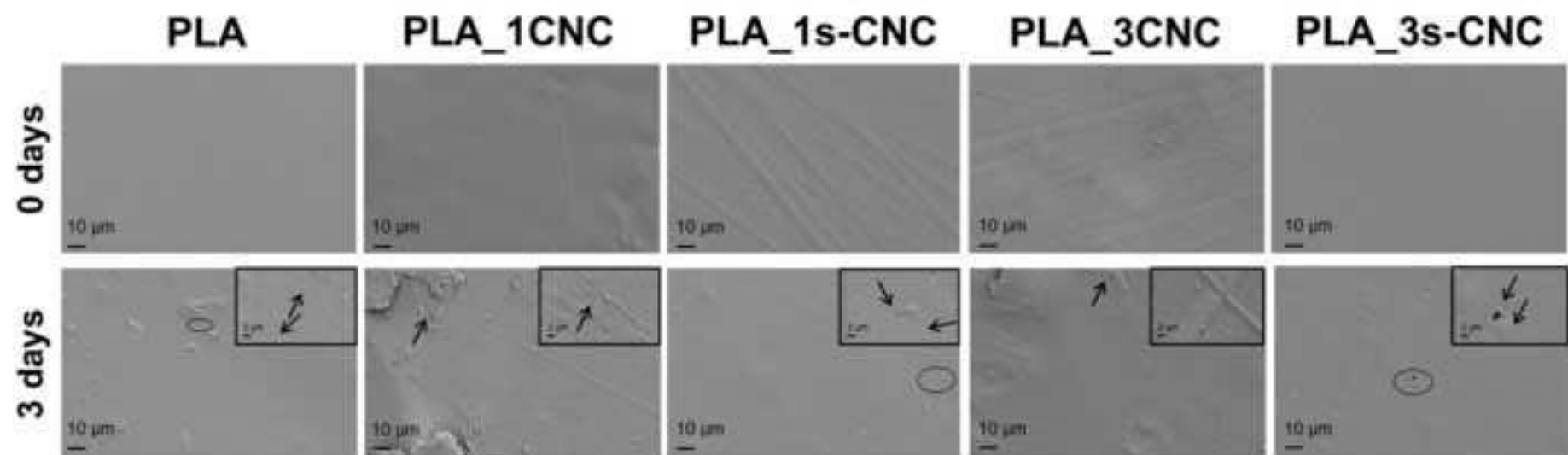**Figure 4**

Figure 5
Click here to download high resolution image
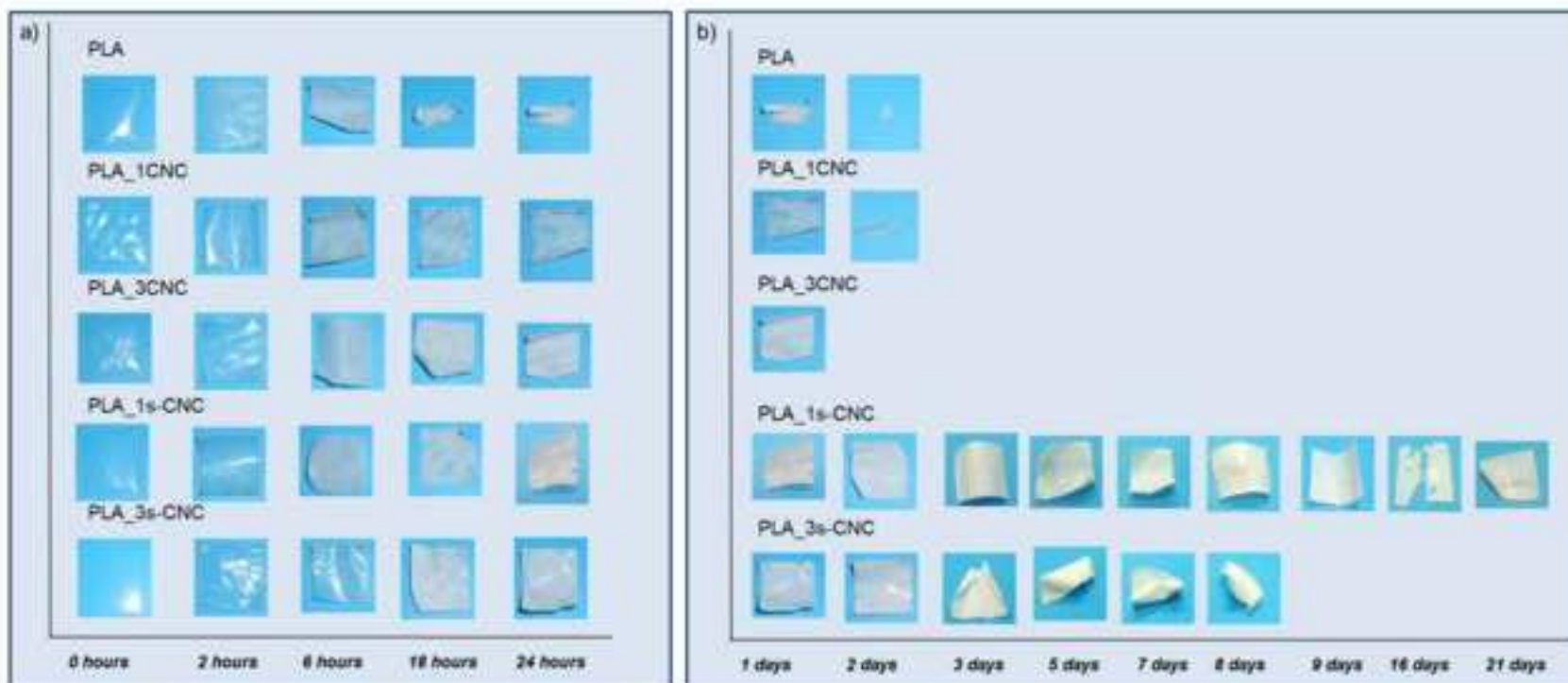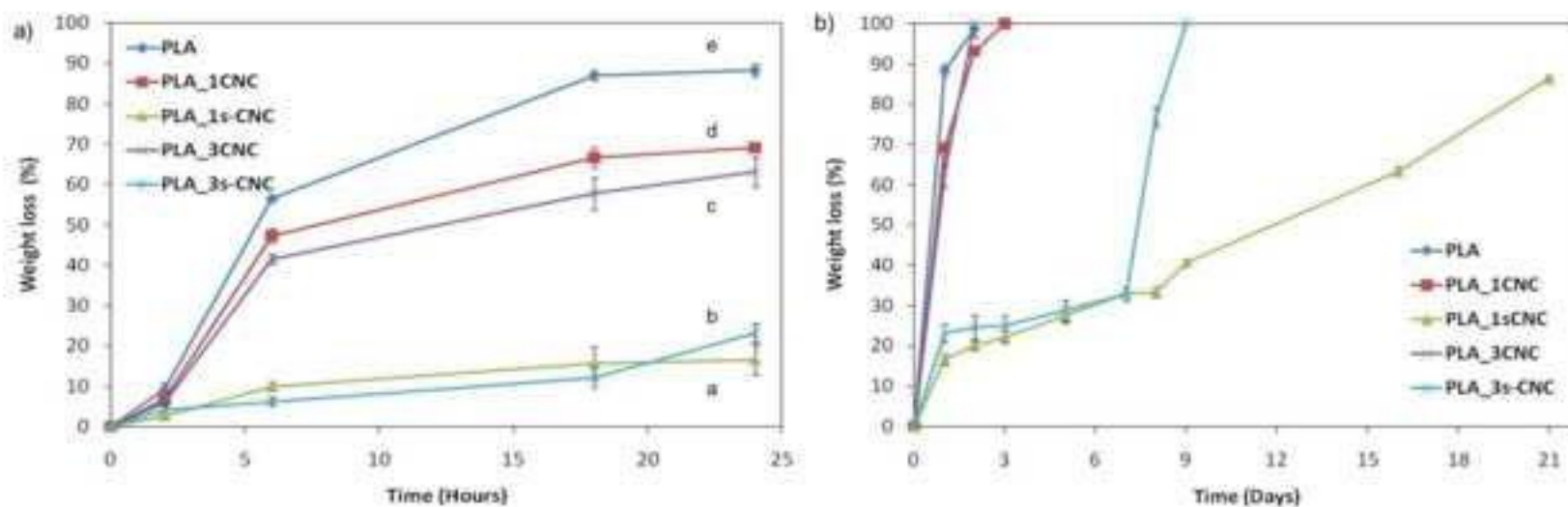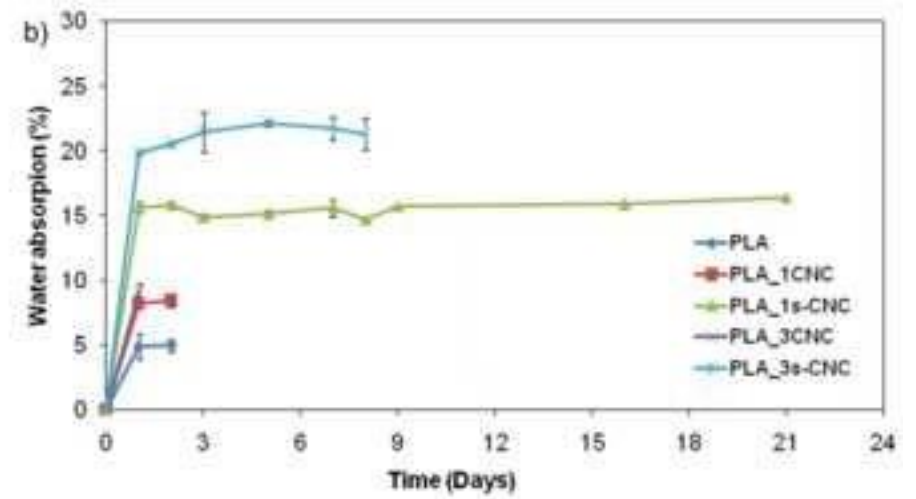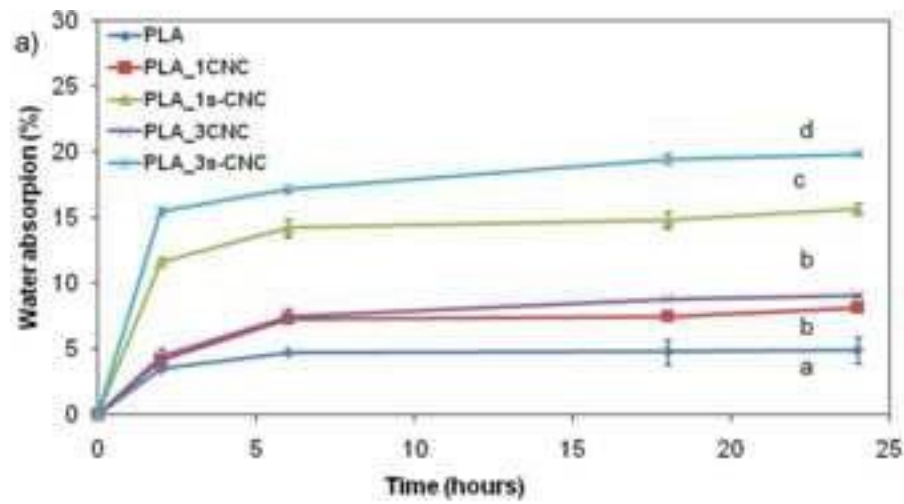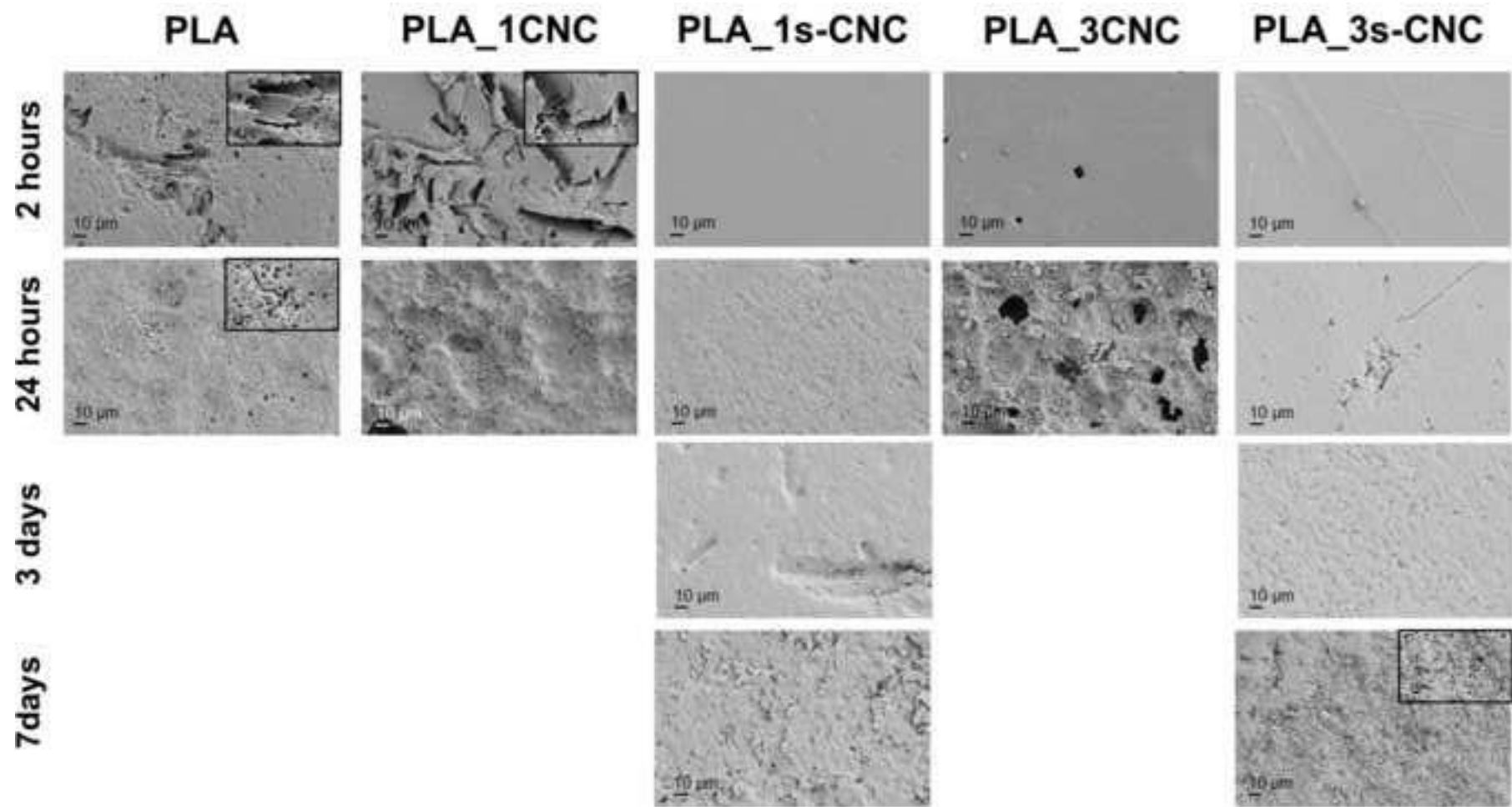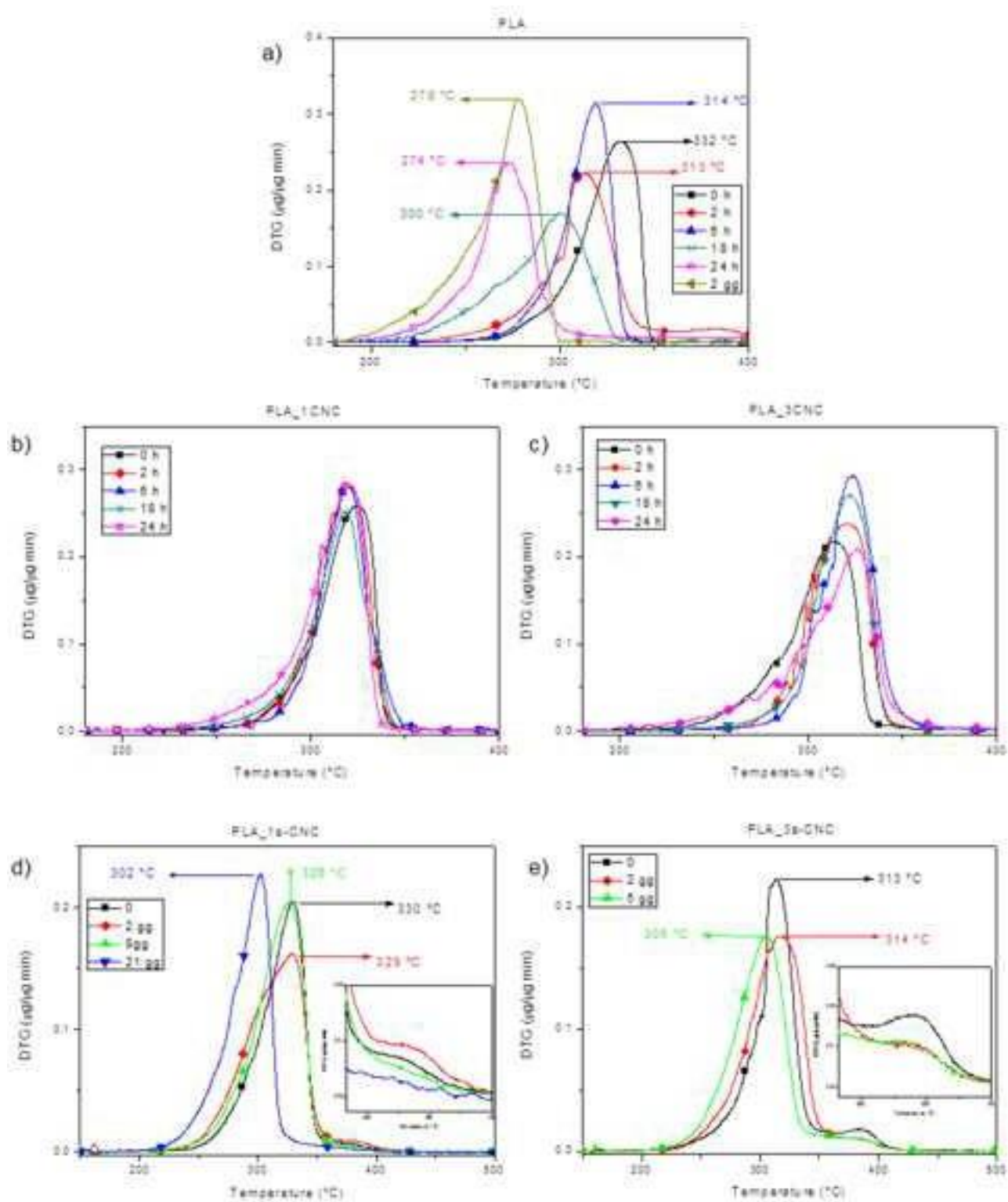
Figure 6
Click here to download high resolution image